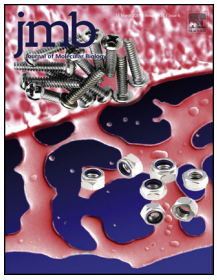

Regulation of Monoamine Oxidase B Gene Expression: Key Roles for Transcription Factors Sp1, Egr1 and CREB, and microRNAs miR-300 and miR-1224

Vikas Arige [1], Anshu Agarwal [1], Abrar A. Khan [1], Ananthamohan Kalyani [1], Bhargavi Natarajan [1], Vinayak Gupta [1], S. Santosh Reddy [2,3], Manoj K. Barthwal [2] and Nitish R. Mahapatra [1]

1 - Department of Biotechnology, *Bhupat and Jyoti Mehta School of Biosciences, Indian Institute of Technology Madras, Chennai 600036, India*

2 - Pharmacology Division, *CSIR—Central Drug Research Institute, Lucknow 226031, India*

3 - Academy of Scientific and Innovative Research (AcSIR), *New Delhi 110025, India*

Correspondence to Nitish R. Mahapatra: *nmahapatra@iitm.ac.in*

https://doi.org/10.1016/j.jmb.2019.01.042

Edited by M Yaniv

Abstract

Monoamine oxidase B (MAO-B), a flavoenzyme located in the outer mitochondrial membrane, is involved in the catabolism of monoamines. Altered levels of MAO-B are associated with cardiovascular/neuronal diseases. However, molecular mechanisms of *MAO-B* gene regulation are partially understood. We undertook a systematic analysis of the *MAO-B* gene to identify the key transcriptional/post-transcriptional regulatory molecules. Expression of *MAO-B* promoter–reporter constructs in cultured cells identified the −144/+25-bp domain as the core promoter region. Stringent *in silico* analysis of this core promoter predicted binding sites for several transcription factors. Over-expression/down-regulation of transcription factors Sp1/Egr1/CREB increased/decreased the *MAO-B* promoter–reporter activity and endogenous MAO-B protein level. Electrophoretic mobility shift assays and ChIP assays provided evidence for interactions of Sp1/Egr1/CREB with the *MAO-B* promoter. *MAOB* transcript level also positively correlated with the transcript level of Sp1/Egr1/CREB in various human tissue samples. Computational predictions using multiple algorithms coupled with systematic functional analysis revealed direct interactions of the microRNAs miR-1224 and miR-300 with *MAO-B* 3′-UTR. Dopamine dose-dependently enhanced *MAO-B* transcript and protein levels *via* increased binding of CREB to *MAO-B* promoter and reduced miR-1224/miR-300 levels. 8-Bromo-cAMP and forskolin augmented *MAO-B* expression, whereas inhibition of PKA diminished the gene expression suggesting involvement of cAMP-PKA axis. Interestingly, Sp1/Egr1/CREB/miR-1224 levels correlate with *MAO-B* expression in rodent models of hypertension/MPTP-induced neurodegeneration, indicating their roles in governing *MAO-B* gene expression in these disease states. Taken together, this study elucidates the previously unknown roles of the transcription factors Sp1/Egr1/CREB and microRNAs miR-1224/miR-300 in regulating *MAO-B* gene expression under basal/disease states involving dysregulated catecholamine levels.

Introduction

Monoamine oxidases (MAO-A and MAO-B) are a family of ubiquitously expressed flavoenzymes localized to the outer mitochondrial membrane and are involved in the oxidative deamination of monoamines. The genes encoding these enzymes lie adjacent to each other on the X chromosome. MAOs are involved in the degradation of monoamines including dopamine which primarily acts *via* the cAMP-PKA-CREB axis [1–3]. In addition, recent studies highlight the role of MAO-B in the synthesis of gamma-aminobutyric acid (GABA), an inhibitory neurotransmitter, from putrescine [4,5]. During development, MAO-A activity appears prior to MAO-B and the activity does not change much with age. Contrary to MAO-A, the enzymatic activity, and mRNA and protein levels of MAO-B tend to increase with age, which in turn leads to enhanced generation of free radicals and subsequent oxidative stress/neurodegeneration [6–8].

MAO-B knockout mice display elevated level of phenylethylamine and increased reactivity to stress [9]. MAO-B level is also elevated in certain neurodegenerative diseases like Parkinson's [10], Alzheimer's [4,11],

multiple-system atrophy, and progressive supranuclear palsy [12]. However, the activity of MAO-B is reduced in smokers, and they are less susceptible to Parkinson's disease (PD) [13]. A transgenic mouse generated to specifically induce MAO-B expression in astrocytes could mimic several key features associated with PD [14]. Administration of L-deprenyl to patients suffering from PD and Alzheimer's disease is beneficial, and it prevents parkinsonism induced in rodents by administration of neurotoxin 1-methyl-4-phenyl-1,2,3,6-tetrahydropyridine (MPTP) [15–17]. Furthermore, the expression of MAO-B is reduced in beta cells of type 2 diabetic patients and db/db mice [18,19]. On the other hand, under chronic hemodynamic stress, the activity of MAO-B is enhanced leading to changes in cardiac structure and function [20]. Thus, altered levels of MAO-B are associated with various cardiovascular and neuronal disease conditions. However, the molecular mechanisms of MAO-B gene regulation remain incompletely understood. Human MAO-B gene expression has been reported to be regulated by TIEG-2 (transforming growth factor-beta-inducible early growth response protein 2) [21], Egr1, c-Jun [22], and specificity proteins Sp1/Sp3/Sp4 [23,24]. We hypothesized that additional transcription factors might be involved in the regulation of MAO-B under basal and pathophysiological conditions.

Micro-RNAs (miRNAs) are small non-coding RNAs which have emerged as important regulators of gene expression *via* binding to the 3′-untranslated region (3′-UTR) of mRNA leading to mRNA degradation or translational inhibition. Altered levels of miRNAs are associated with a variety of disorders including cardiovascular diseases [25] and neuronal disorders [26]. The role of miRNAs in MAO-B gene regulation, however, remains unexplored. We hypothesized that MAO-B might be regulated by certain miRNAs at the post-transcription level. Accordingly, we undertook systematic computational and experimental analyses that revealed previously unknown roles of a proximal promoter domain (−144/−78 bp) in *cis* and the transcription factors Sp1/Egr1/CREB in *trans* to govern the expression of MAO-B under basal and dopamine-induced conditions. In addition, this study, for the first time, provides evidence for regulation of MAO-B by miR-1224/miR-300. This study also demonstrated significant correlations between these molecular regulators and MAO-B expression in various human tissues as well as in rodent models of essential hypertension.

Results

Identification of crucial promoter motifs governing MAO-B gene expression

In order to identify the proximal promoter domains (*cis*-elements) that may govern MAO-B gene expression, a series of progressive mouse MAO-B 5′-promoter deletion–reporter constructs (carrying −1473, −1034, −695, −346, −286, −144, and −77 bp to +25-bp regions) and the promoter-less pGL3-basic (as negative control) were transfected into HEK-293, N2a, AGS, CHO, AML 12, and IMR-32 cell lines (Fig. 1). Progressive deletion of the promoter region from −1473 bp caused gradual enhancement in luciferase activity till −144 bp, but further deletion to −77 bp significantly reduced luciferase activity in all the tested cell lines: 7.2-fold in HEK-293 (one-way ANOVA: $F = 90.35$, $p < 0.0001$), 3.3-fold in N2a (one-way ANOVA: $F = 50.44$, $p < 0.0001$), 5.6-fold in AGS (one-way ANOVA: $F = 13.42$, $p < 0.0001$), 3.0-fold in CHO (one-way ANOVA: $F = 12.19$, $p < 0.0001$), 2.5-fold in AML 12 (one-way ANOVA: $F = 49.75$, $p < 0.0001$), and 6.5-fold in IMR-32 (one-way ANOVA: $F = 38.31$, $p < 0.0001$). Thus, the −144- to −78-bp region appears to be crucial for basal expression of MAO-B in various cell types. Hence, subsequent experiments were carried out utilizing the MAOB–pro-144 construct. A stringent analysis of the proximal promoter region of MAO-B using *in silico* tools (*viz.* ConSite, PROMO, and MatInspector) predicted putative binding sites for Sp1 (at −108/−99 bp and −45/−36 bp), Egr1 (at −108/−99 bp), CREB (at −130/−119 bp and −81/−70 bp), and AP2alpha (at −62/−54 bp) by at least two of these programs (Fig. S1A), suggesting that the expression of MAO-B gene may be regulated by these transcription factors. Interestingly, alignment of the mouse, rat, and human MAO-B promoters revealed that the binding sites for Sp1, Egr1, and CREB are highly conserved across these species; on the other hand, the binding site for AP2alpha was only partially conserved among these mammals (Fig. S1B).

Role of Sp1, Egr1, and CREB in MAO-B transcriptional regulation

To ascertain the roles of the *in silico* predicted transcription factors (*viz.* Sp1, Egr1, CREB, and AP2alpha) in MAO-B gene regulation, we measured the MAO-B promoter activity by modulating the levels/binding of these transcription factors. Co-transfection of the MAOB–pro-144 construct with Sp1, or Egr1, or CREB expression plasmid dose-dependently augmented the MAO-B promoter activities (one-way ANOVA: $F = 34.31$, up to 2.5-fold, $p < 0.0001$; one-way ANOVA: $F = 40.29$, up to 4.1-fold, $p < 0.0001$; or one-way ANOVA: $F = 25.83$, up to 5.4-fold, $p < 0.001$, respectively) (Fig. 2b–d). Conversely, co-transfection of the MAOB–pro-144 construct with increasing doses of Sp1-shRNA, Egr1-shRNA plasmid, or K-CREB plasmid dose-dependently diminished the MAO-B promoter activities (one-way ANOVA: $F = 866.2$, up to 125-fold, $p < 0.0001$; one-way ANOVA: $F = 29.29$, up to 3.6-fold, $p < 0.0001$; or one-way ANOVA: $F = 18.1$, up to 20-fold, $p < 0.001$, respectively) (Fig. 2e–g). The

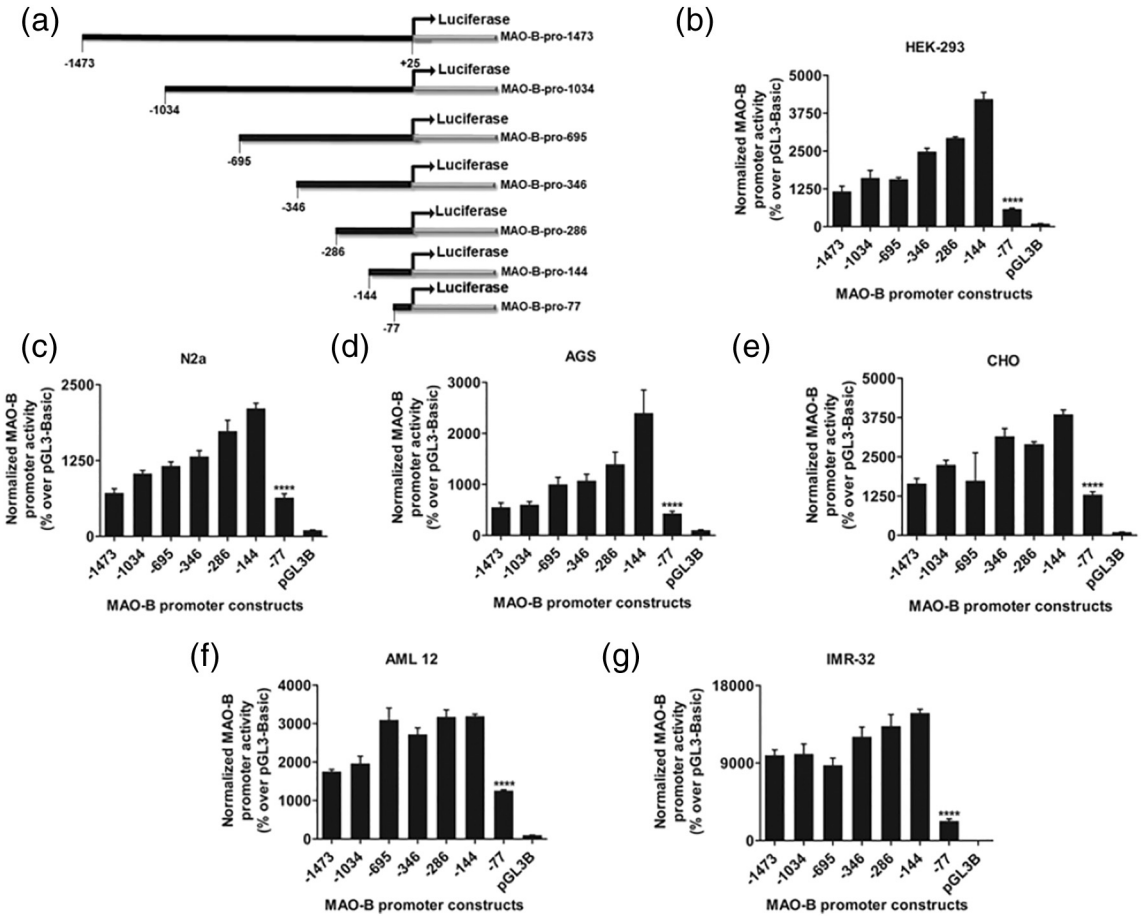

Fig. 1. Identification of crucial *cis*-elements in the mouse MAO-B promoter. (a) Schematic representation of MAO-B promoter deletion constructs generated by cloning into pGL3-Basic vector. (b-g) The promoter–reporter constructs or pGL3-Basic vector were co-transfected with pCMV-β-galactosidase expression plasmid as transfection control for normalization of promoter activities into HEK-293 (b), N2a (c), AGS (d), CHO (e), AML 12 (f), and IMR-32 (g). Promoter activities were normalized with β-galactosidase, and the results are expressed as percentage over pGL3-Basic. The results are mean ± SE of triplicate values. Statistical significance was determined by one-way ANOVA with Bonferroni's multiple comparisons post-test. ****$p < 0.0001$ as compared to MAOB–pro-144 construct.

over-expression of Sp1, Egr1, and CREB (Fig. 2b–d) and down-regulation of Sp1 and Egr1 (Fig. 2e, f) were confirmed by Western blotting. In addition to the promoter activity, over-expression/down-regulation of Sp1, Egr1, and CREB also resulted in a dose-dependent increase/decrease in the endogenous MAO-B protein levels (Fig. 2b–g). In corroboration, down-regulation of endogenous CREB by CREB-siRNA (confirmed by Western blotting) decreased the promoter activity (Fig. S2A). On the contrary, co-transfection of MAO-B promoter construct with varying amounts of AP2alpha expression plasmid did not result in significant change in the promoter activity (Fig. S2B), suggesting that AP2alpha may not regulate MAO-B expression. Together, these results indicate important roles for Sp1, Egr1, and CREB in regulating MAO-B gene expression under basal conditions.

To evaluate if Sp1, Egr1, and CREB act in concert to regulate MAO-B gene expression, the MAO-B promoter construct was co-transfected with various combinations of Sp1, Egr1, and CREB expression plasmids. Sp1 and Egr1 individually enhanced the promoter activity by ~1.4-fold ($p < 0.01$) and ~2.7-fold ($p < 0.0001$), respectively; the combination of both Sp1 and Egr1 did not yield any additive/synergistic effect in line with the *in silico* prediction that Sp1 and Egr1 have a common binding site in the MAO-B proximal promoter. Co-transfection of MAO-B promoter with CREB augmented the promoter activity by ~11.3-fold ($p < 0.05$), whereas CREB together with Sp1 or Egr1 caused a further enhancement in promoter activity by ~21.3-fold ($p < 0.0001$) or ~26.3-fold ($p < 0.0001$). Furthermore, together Sp1, Egr1, and CREB augmented the promoter activity

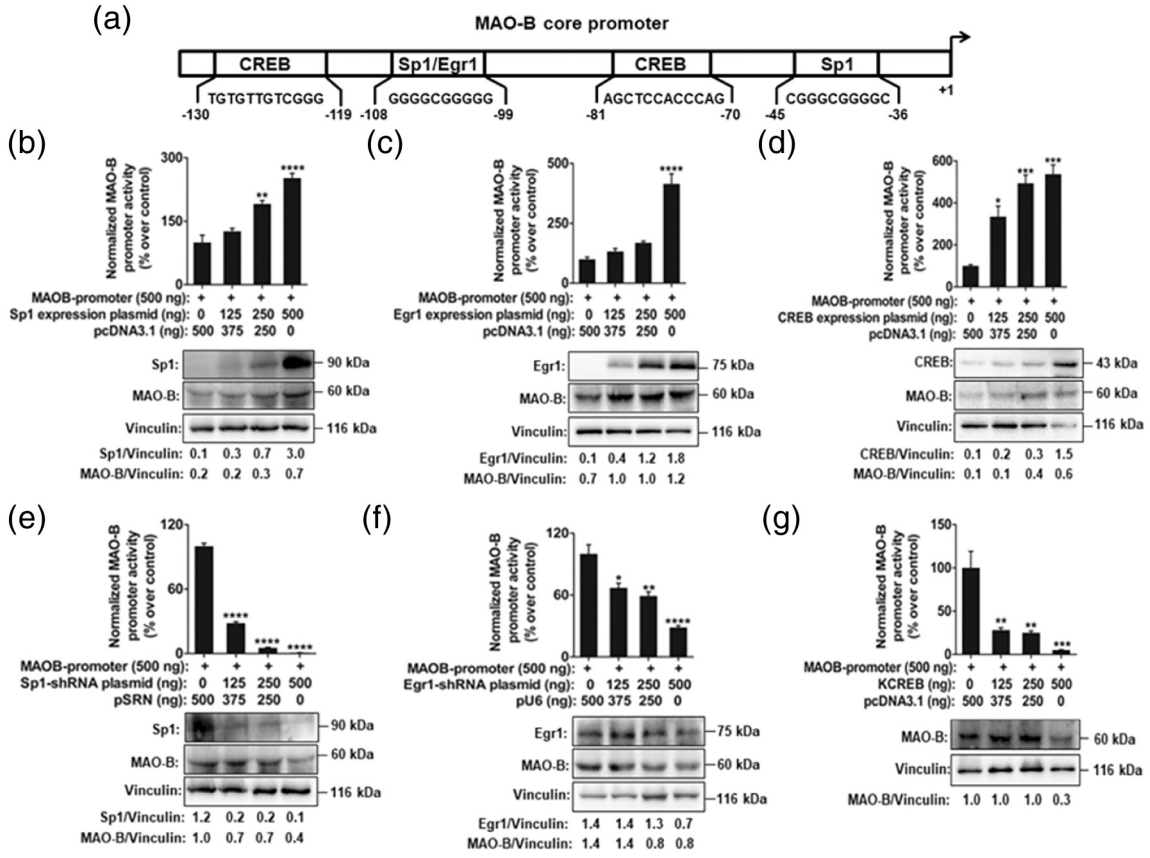

Fig. 2. Role of Sp1/Egr1/CREB on the MAO-B promoter activity and protein levels. (a) Schematic representation of Sp1, Egr1, and CREB binding sites in the MAO-B promoter. MAO-B promoter–reporter construct was co-transfected with increasing doses of Sp1 (b), Egr1 (c), and CREB (d) expression plasmid into N2a cells. Over-expressions of Sp1, Egr1, CREB, and endogenous increase in MAO-B protein levels were confirmed by Western blotting. MAO-B promoter–reporter construct was co-transfected with increasing doses of Sp1-shRNA (e), Egr1-shRNA expression plasmid (f) or with KCREB plasmid (g). Down-regulations of Sp1, Egr1, and endogenous decrease in MAO-B protein levels were confirmed by Western blotting. Relative levels of Sp1, Egr1, CREB, and MAO-B after normalization with vinculin are shown. For promoter–reporter assays, the promoter activities were normalized with total protein and the results are expressed as percentage over control. The results are mean ± SE of triplicate values. Statistical significance was determined by one-way ANOVA with Bonferroni's multiple comparisons post-test. *$p < 0.05$, **$p < 0.01$, ***$p < 0.001$, ****$p < 0.0001$ with respect to basal MAOB-promoter activity.

by ~42.2-fold ($p < 0.0001$; Fig. S3). These results suggest synergistic action of Sp1, Egr1, and CREB to regulate MAO-B gene expression.

Effect of mutations at Sp1/Egr1 and CREB binding sites on MAO-B promoter activity

To further validate whether Sp1, Egr1, and CREB interact with the MAO-B promoter domains, mutations were generated at the transcription factor binding sites. The wild-type or mutant promoter constructs were co-transfected with increasing amounts of Sp1, Egr1, or CREB expression plasmid. Co-transfection of the wild-type promoter construct with Sp1, Egr1, or CREB expression plasmid dose-dependently augmented the promoter activities (up to 8.1-fold, $p < 0.0001$; 15.5-fold, $p < 0.001$; or 120-fold, $p < 0.0001$, respectively) (Fig. 3a–c). On the other hand, co-transfection of the mutant promoter constructs lacking the Sp1, Egr1, or CREB binding site with Sp1, Egr1, or CREB expression plasmid led to drastically diminished response in reporter activities (up to 49-fold, $p < 0.0001$; 128-fold, $p < 0.0001$; or 3-fold, $p < 0.0001$, respectively) (Fig. 3a–c). Thus, the *cis*-elements predicted by the transcription factor prediction tools appear to be functional and could be the actual binding sites for Sp1, Egr1, and CREB. In each case, the over-expression of transcription factors was confirmed by Western blotting.

In vitro interactions of Sp1, Egr1, and CREB with the MAO-B promoter: electrophoretic mobility shift assays

In order to test the binding of Sp1/Egr1/CREB with MAO-B promoter, we carried out electrophoretic

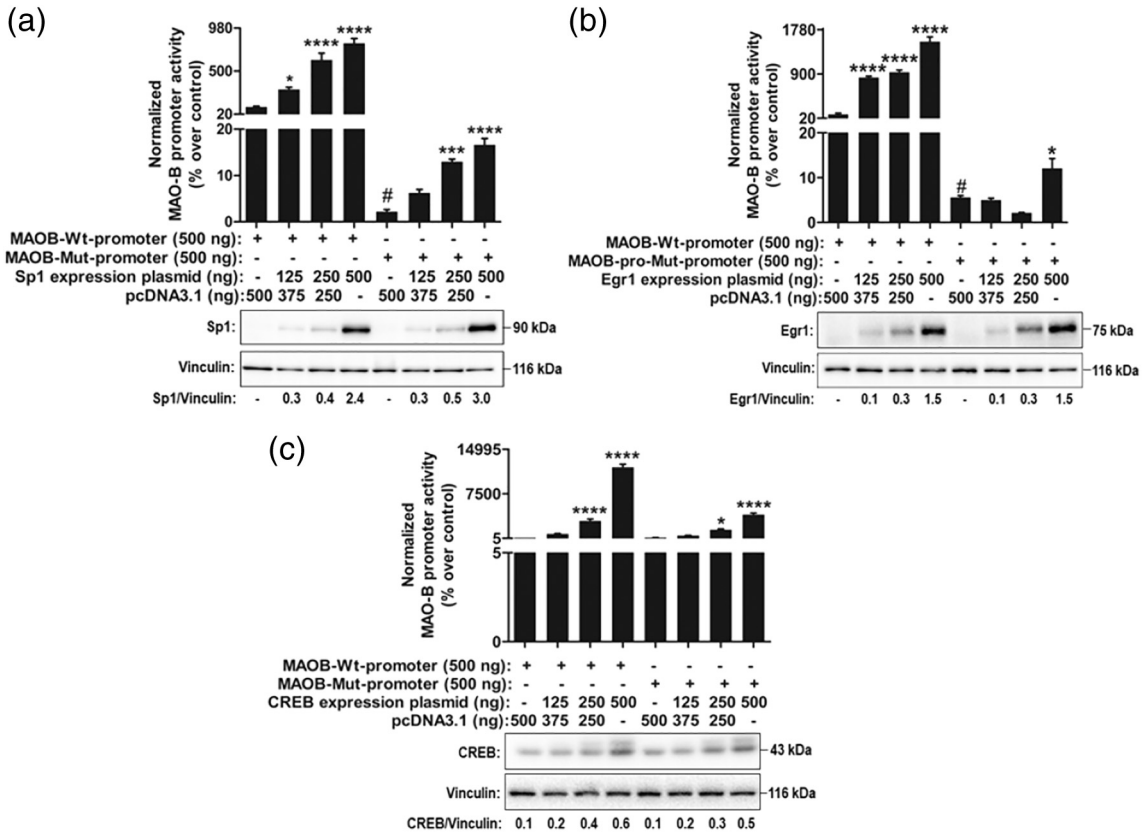

Fig. 3. Functional validation of Sp1/Egr1/CREB binding sites in the MAO-B proximal promoter domain. MAO-B wild-type or mutant promoter–reporter construct were co-transfected with increasing doses of Sp1 (a), Egr1 (b), and CREB (c) expression plasmid into N2a cells. Promoter activities were normalized with total protein, and the results are expressed as percentage over control. The results are mean ± SE of triplicate values. Statistical significance was determined by one-way ANOVA with Bonferroni's multiple comparisons post-test. $^{*}p < 0.05$, $^{**}p < 0.01$, $^{***}p < 0.001$, $^{****}p < 0.0001$ with respect to basal MAO-B promoter activity. $^{\#}p < 0.001$, with respect to wild-type promoter activity. Over-expressions of Sp1, Egr1, and CREB were confirmed by Western blotting. Relative levels of Sp1, Egr1, and CREB after normalization with vinculin are shown.

mobility shift assay (EMSA). Incubation of nuclear protein extract from N2a cells with either the wild-type oligo (harboring binding sites for Sp1/Egr1) or mutant oligo (carrying mutations at the Sp1/Egr1 binding site) (Fig. 4a) yielded several DNA–protein complexes. The wild-type Sp1/Egr1 oligo yielded a specific complex (lanes 4, Fig. 4b) as opposed to the mutant Sp1/Egr1 oligo (lanes 2, Fig. 4b). Moreover, addition of excess unlabeled wild-type Sp1/Egr1 oligo caused a gradual dose-dependent decline in the intensity of the specific band (lanes 5–7, Fig. 4b); in contrast, the intensity of the specific band remained unaffected upon addition of excess unlabeled mutant Sp1/Egr1 oligo (lanes 8–10, Fig. 4b). Furthermore, to verify the involvement of these transcription factors in the formation of specific complexes, antibodies against Sp1 and Egr1 were added to nuclear protein isolated from N2a cells transfected with either Sp1 expression plasmid or Egr1 expression plasmid. The intensity of the specific complex diminished upon the addition of anti-Sp1/anti-Egr1 antibody (lane 2, Fig. 4c, d). As a control in these reactions (lane 3, Fig. 4c, d) IgG was used, which did not alter the intensity of the specific band. Thus, Sp1 and Egr1 appear to interact with the MAO-B promoter *in vitro*.

We also carried out EMSA to assess the *in vitro* interaction of CREB with the MAO-B promoter (Fig. 4e). Incubation of biotin-labeled CREB binding site harboring wild-type oligo with nuclear protein extract from N2a yielded a specific complex (lane 4, Fig. 4f), whereas incubation of biotin-labeled oligos with mutated or deleted CREB binding site and nuclear protein extract from N2a did not result in specific complex formation (lanes 5 and 6, Fig. 4f). Furthermore, to determine the involvement of CREB in formation of the specific complex, an antibody against CREB was added to the reaction mixture. Addition of CREB antibody in the reaction mixture led to decrease in intensity of the specific band (lanes 2 and 3, Fig. 4g). We also used IgG as a control which did not interfere with the intensity of

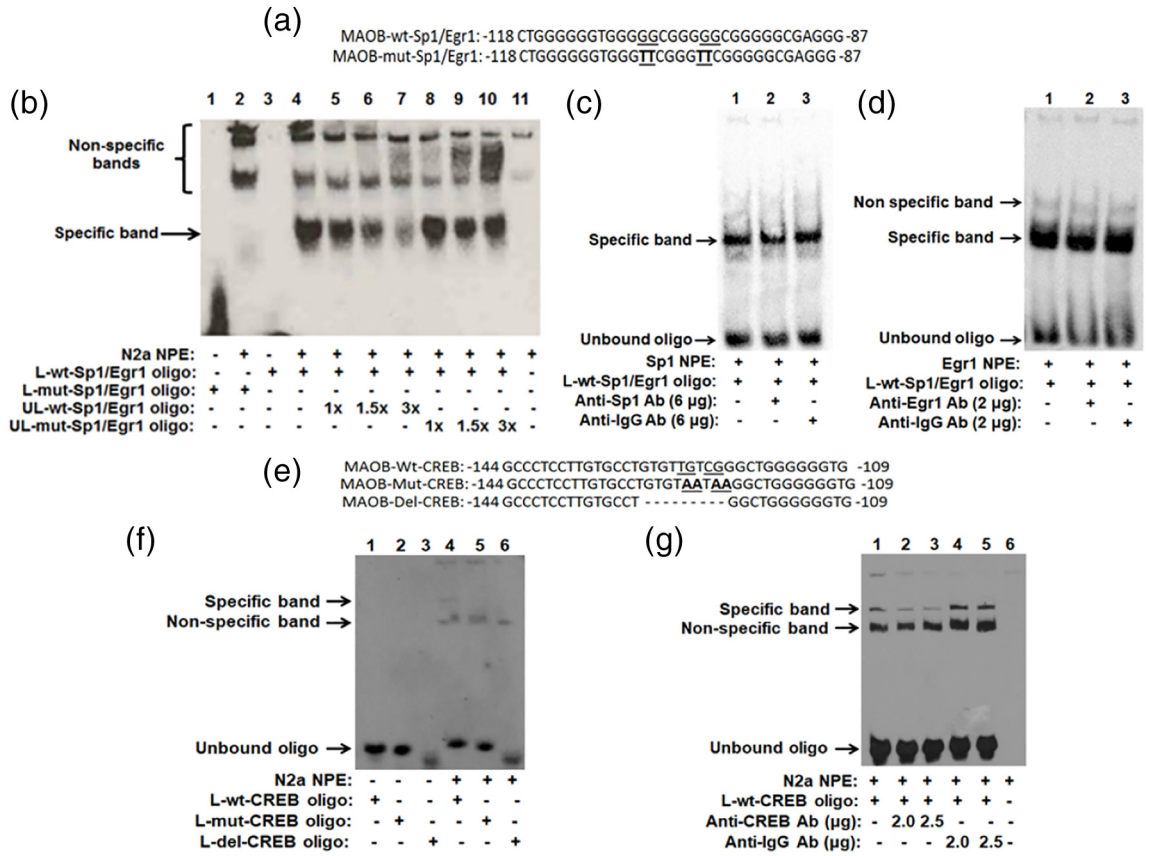

Fig. 4. Sp1, Egr1, and CREB interact with the proximal MAO-B promoter *in vitro*. (a) Sequence of wild-type and mutant Sp1/Egr1 oligos. (b) EMSA for Sp1/Egr1: Lane 1, Biotin-labeled Sp1/Egr1 mutant oligo. Lane 2, N2a NPE incubated with labeled Sp1/Egr1 mutant oligo. Lanes 3, Biotin-labeled Sp1/Egr1 wild-type oligo. Lane 4, N2a NPE incubated with labeled Sp1/Egr1 wild-type oligo. Lanes 5–7, N2a NPE incubated with labeled Sp1/Egr1 wild-type oligo along with molar excesses of unlabeled wild-type oligo. Lanes 8–10, N2a NPE incubated with labeled Sp1/Egr1 wild-type oligo along with molar excesses of unlabeled mutant oligo. Lane 11, N2a NPE. (c) Antibody interference assay using Sp1 antibody. Lane 1, NPE from Sp1 over-expressing N2a cells (Sp1 NPE) incubated with labeled Sp1/Egr1 wild-type oligo. Lane 2, Sp1 NPE incubated with labeled Sp1/Egr1 wild-type oligo and anti-Sp1 antibody. Lane 3, Sp1 NPE incubated with labeled Sp1/Egr1 wild-type oligo and anti-IgG antibody. (d) Antibody interference assay using Egr1 antibody. Lane 1, NPE from Egr1 over-expressing N2a cells (Egr1 NPE) incubated with labeled Sp1/Egr1 wild-type oligo. Lane 2, Egr1 NPE incubated with labeled Sp1/Egr1 wild-type oligo and anti-Egr1 antibody. Lane 3, Egr1 NPE incubated with labeled Sp1/Egr1 wild-type oligo and anti-IgG antibody. (e) Sequence of wild-type, mutant, and CREB deletion oligos. (f) EMSA for CREB: Lane 1, Biotin-labeled CREB wild-type oligo. Lane 2, Biotin-labeled CREB mutant oligo. Lane 3, Biotin-labeled CREB site deleted oligo. Lane 4, N2a NPE incubated with labeled CREB wild-type oligo. Lane 5, N2a NPE incubated with labeled CREB mutant oligo. Lane 6, N2a NPE incubated with labeled CREB site deleted oligo. (g) Antibody interference assay using CREB antibody. Lane 1, N2a NPE incubated with labeled CREB wild-type oligo, Lanes 2–3, N2a NPE incubated with labeled CREB wild-type oligo and anti-CREB antibody, Lanes 4–5, N2a NPE incubated with labeled CREB wild-type oligo and anti-IgG antibody, Lane 6, N2a NPE. NPE, nuclear protein extract; wt, wild type; mut, mutant; L, labeled; UL, unlabeled; del, deletion.

the specific complex (lanes 4 and 5, Fig. 4g). These results provide evidence for *in vitro* interaction of CREB with the MAO-B proximal promoter.

Binding of Sp1, Egr1, and CREB with the endogenous MAO-B promoter: chromatin immunoprecipitation assays

In view of our findings on interactions of Sp1, Egr1, and CREB with the MAO-B promoter, we next investigated whether these transcription factors bind to the endogenous MAO-B promoter in the context of chromatin *in vivo* using chromatin immunoprecipitation (ChIP) assays. Antibodies specific to Sp1, Egr1, and CREB were used to precipitate formaldehyde cross-linked chromatin fragments from N2a cells. DNA isolated from Sp1/Egr1/CREB immunoprecipitated lysates yielded a ~224-bp PCR product encompassing the MAO-B promoter domain (−144 bp/+82 bp) that harbored binding sites for these transcription factors (lanes 3–5, Fig. 5b). As a positive control, input DNA gave a similar size amplicon (lane 2, Fig. 5b), while as a

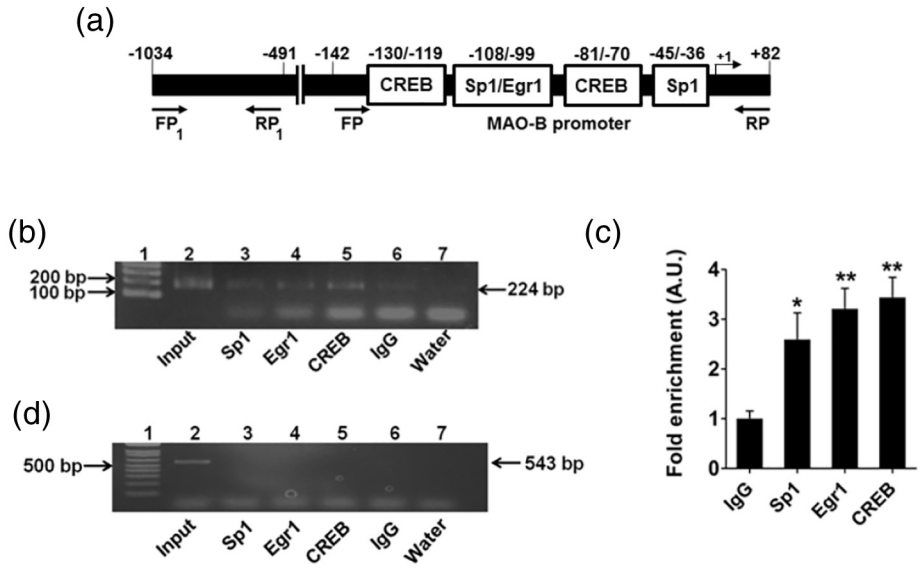

Fig. 5. Sp1, Egr1, and CREB interact with the MAO-B core promoter *in vivo* in the context of chromatin. (a) Schematic representation of Sp1, Egr1, and CREB binding sites in the MAO-B promoter and strategy employed for primer designing. (b) End-point PCR using immunoprecipitated chromatin and specific primers. Input DNA served as positive control; IgG and water served as negative for immunoprecipitation and end-point PCR, respectively. (c) Real-time PCR depicting fold enrichment over IgG. Statistical significance was determined by one-way ANOVA with Bonferroni's multiple comparisons post-test. *$p < 0.05$, **$p < 0.01$ with respect to IgG. (d) End-point PCR using primers specific to the MAO-B promoter outside the Sp1, Egr1, and CREB binding domain did not result in any amplification confirming specificity of ChIP. Input was used as positive control, while water was used as negative control for PCR.

negative control, pre-immune IgG-precipitated chromatin did not yield significant amplification indicating specificity of the immunoprecipitation reactions (lane 6, Fig. 5b). As a negative control for PCR, water was used instead of the immunoprecipitated DNA, which did not result in amplification (lane 7, Fig. 5b). Next, qPCR was carried out using the same immunoprecipitated DNA, and there was a significant enrichment of MAO-B promoter domain with Sp1, Egr1, or CREB antibody (up to 2.6-fold, $p < 0.05$; 3.2-fold, $p < 0.01$; or 3.5-fold, $p < 0.01$, respectively) as compared to pre-immune IgG immunoprecipitated chromatin (Fig. 5c). Another primer pair designed outside the Sp1/Egr1/CREB domain gave amplification with input chromatin (lane 2, Fig. 5d), but did not yield amplification with the immunoprecipitated DNA confirming the specificity of ChIP assays (lanes 3–6, Fig. 5d). These results provide evidence for endogenous interaction of Sp1, Egr1, and CREB with the MAO-B promoter domain.

Prediction of putative miRNA binding sites in the mouse MAO-B 3′-UTR

Since the role of miRNAs in regulating MAO-B gene expression remains unknown, we utilized various *in silico* miRNA binding site prediction tools to predict the putative miRNAs that might interact with the MAO-B 3′-UTR. miRNAs predicted by at least four different programs were short-listed (Table S5) for further consideration. Based on thermodynamic values (i.e., ΔG and $\Delta\Delta G$ obtained using RNAhybrid and PITA), we choose to validate the roles of mmu-miR-532-3p, mmu-miR-300-3p, and mmu-miR-1224-5p, which appeared to have the highest affinities for the MAO-B 3′-UTR.

Effect of over-expression of microRNAs, mimics, and inhibitors on the endogenous MAO-B protein levels

In order to validate the roles of these *in silico* predicted miRNAs, the MAO-B 3′-UTR reporter construct was co-transfected with increasing amounts of either the miR-1224 or miR-300 or miR-532 expression plasmid into N2a cells. There was a dose-dependent decrease in the MAO-B 3′-UTR reporter activity with increasing amounts of miR-1224 (one-way ANOVA: $F = 303.7$, up to 2.1-fold, $p < 0.0001$) or miR-300 (one-way ANOVA: $F = 56.99$, 2.0-fold, $p < 0.0001$) (Fig. 6a and b); such a decrease in the reporter activity was not observed with miR-532 expression plasmid (Fig. S4A). The over-expression of miR-1224, miR-300 (Fig. 6c, d), and miR-532 (Fig. S4B) was confirmed by real-time PCR. In addition

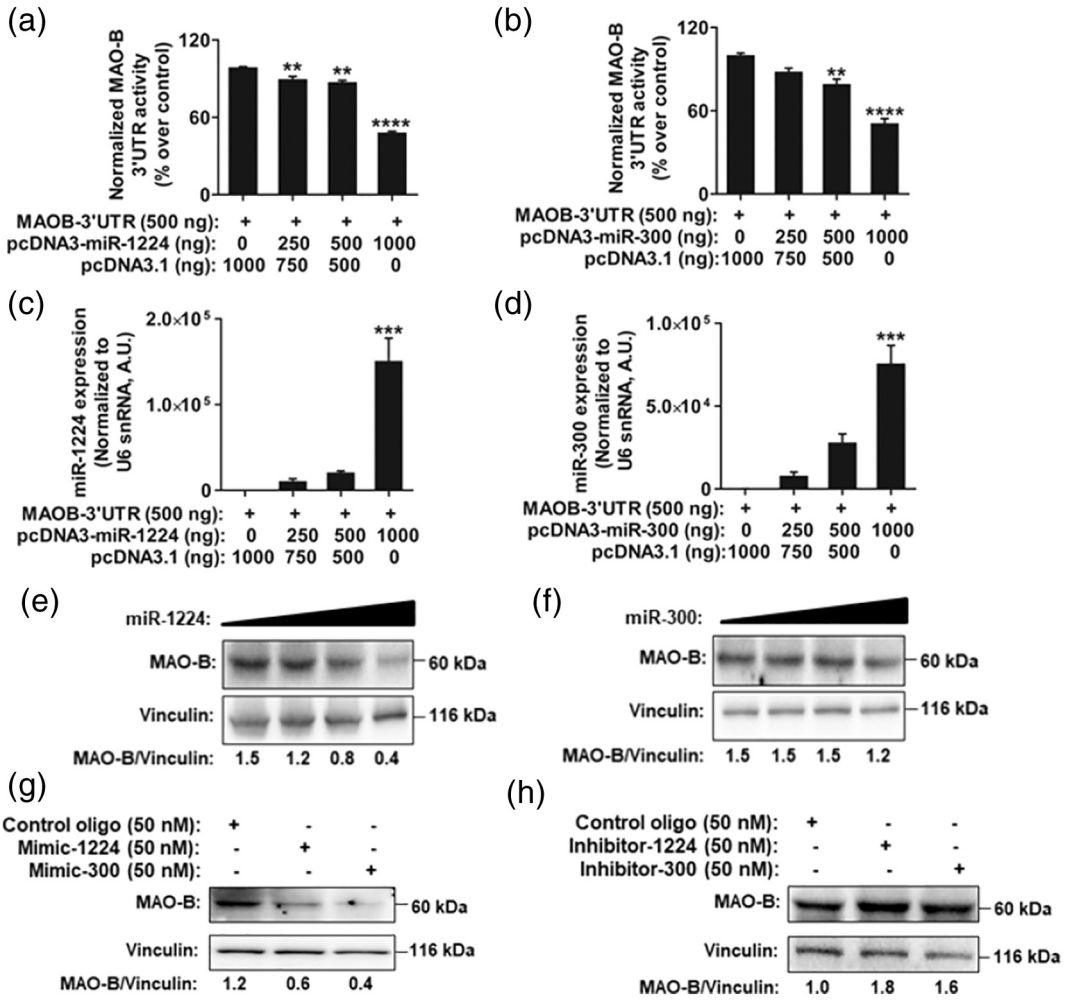

Fig. 6. miR-1224 and miR-300 dampen MAO-B gene expression. Co-transfection of MAO-B 3′-UTR with increasing doses of either miR-1224 (a) or miR-300 (b) expression plasmid and pMIR-Report beta-gal control vector into N2a cells resulted in a dose-dependent decrease in the reporter activity. In both the cases, the reporter activities were normalized to β-galactosidase activity, and the results are expressed as percentage fold change over basal. Total RNA isolated from N2a cells co-transfected with MAO-B 3′-UTR and miR-1224 or miR-300 was reverse transcribed to cDNA. Real-time PCR was carried out to confirm over-expression of miR-1224 (c) and miR-300 (d). All the results are mean ± SE of triplicate values. Statistical significance was determined by one-way ANOVA with Bonferroni's multiple comparisons post-test. $^{**}p < 0.01$, $^{***}p < 0.001$, $^{****}p < 0.0001$ with respect to basal condition. Western blots confirming decrease in MAO-B protein levels upon over-expression of miR-1224 (e) and miR-300 (f). (g) 50 nM miR-1224 mimic or miR-300 mimic transfection into N2a cells diminished the endogenous MAO-B protein levels compared to control oligo. (h) 50 nM miR-1224 antagomir or miR-300 antagomir transfection into N2a cells augmented the endogenous MAO-B protein levels compared to control oligo. Relative levels of MAO-B after normalization with vinculin are shown.

to the reporter activity, the endogenous MAO-B protein levels also decreased upon over-expression of miR-300 and miR-1224 (Fig. 6e, f). In corroboration, the MAO-B protein levels significantly diminished upon transfection of either miR-1224 mimic or miR-300 mimic (50 nM) compared to control oligo (Fig. 6g). We also used miR-1224 or miR-300 inhibitors (50 nM) to quench the endogenous microRNAs. The MAO-B protein levels increased upon transfection of either miR-1224 inhibitor or miR-300 inhibitor compared to control oligo (Fig. 6h). These results demonstrate the roles of miR-300 and miR-1224 in governing MAO-B gene expression at the post-transcriptional level.

Effect of dopamine, forskolin, 8-Br-cAMP, and protein kinase A inhibitor on MAO-B expression

Since MAO-B is involved in the catabolism of dopamine, we sought to test whether dopamine influences MAO-B promoter activity and protein levels. N2a cells transfected with MAO-B promoter were treated with various doses of dopamine. Indeed,

dopamine dose-dependently (one-way ANOVA: $F = 11.25$, up to 2.1-fold, $p < 0.001$) (Fig. 7a) and time-dependently (one-way ANOVA: $F = 25.09$, up to 1.5-fold, $p < 0.0001$) (Fig. 7b) enhanced the MAO-B promoter activity.

As dopamine has been reported to activate expression of several genes *via* augmentation of the intracellular cAMP levels, we tested the effect of forskolin (an activator of adenylate cyclase) [27] and 8-Br-cAMP (a synthetic analogue of cAMP and an activator of PKA) on the MAO-B expression. Forskolin (Fig. 7c) and 8-Br-cAMP (Fig. 7d) treatment resulted in a significant increase in MAO-B promoter activity [one-way ANOVA: $F = 29.07$ (up to 1.7-fold, $p < 0.001$) and one-way ANOVA: $F = 46.58$ (up to 22-fold, $p < 0.0001$), respectively] and endogenous protein levels (Fig. S5).

Consistent with these results, co-transfection of MAO-B promoter with increasing doses of protein kinase A inhibitor (PKI) plasmid resulted in a dose-dependent, significant decrease in the MAO-B promoter activity (one-way ANOVA: $F = 26.13$, up to 5.2-fold, $p < 0.0001$) (Fig. 7e). Moreover, inhibition of endogenous PKA resulted in diminished endogenous MAO-B protein levels (Fig. 7f). Furthermore, dopamine treatment resulted in a significant enhancement in the endogenous MAO-B mRNA levels (24-fold, $p < 0.0001$) (Fig. 7g) and a dose-dependent increase in endogenous MAO-B protein levels (Fig. 7h). These results suggest involvement of adenylate cyclase,

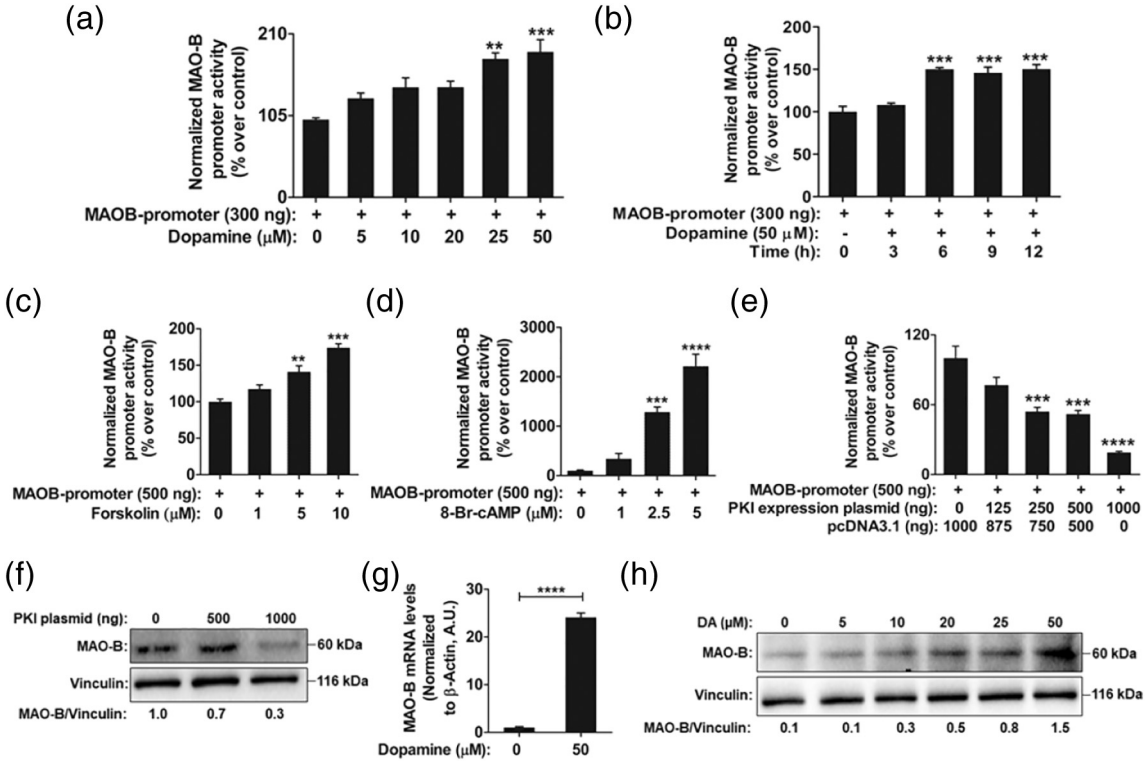

Fig. 7. Dopamine and cyclic AMP activate the expression of MAO-B gene. N2a cells transfected with the MAO-B promoter–reporter construct were treated with increasing concentrations of dopamine (a), with 50 μM dopamine for different time points (b), increasing concentrations of forskolin (c), or 8-bromo-cyclic AMP (d) resulted in a dose-dependent increase in promoter activity. (e) MAO-B promoter–reporter construct co-transfected with increasing concentrations of PKI expression plasmid into N2a cells dose-dependently diminished the promoter activity. In each case, the promoter activity was normalized with total protein, and the results are expressed as percentage over control. The results are mean ± SE of triplicate values. Statistical significance was determined by one-way ANOVA with Bonferroni's multiple comparisons post-test. $^{**}p < 0.01$, $^{***}p < 0.001$, $^{****}p < 0.0001$ with respect to basal MAO-B promoter activity. (f) Western blot depicting decrease in endogenous protein levels of MAO-B upon PKI over-expression. Relative levels of MAO-B after normalization with vinculin are shown. (g) Real-time PCR following exposure to 50 μM dopamine was performed using MAO-B and β-actin gene-specific primers. Statistical significance was determined by Student's *t* test (unpaired, two-tailed). $^{****}p < 0.0001$ with respect to untreated/control. (h) Western blot depicting increase in endogenous protein levels of MAO-B upon treatment with increasing concentration of dopamine. Relative levels of MAO-B after normalization with vinculin are shown.

cAMP and PKA axis leading to augmented MAO-B expression.

Role of miRNAs and CREB in mediating dopamine-induced MAO-B expression

Considering that dopamine up-regulates MAO-B protein levels and based on the observations that miR-1224 and miR-300 are involved in MAO-B gene expression, we quantified the endogenous levels of these miRNAs upon dopamine (50 μM) treatment. Indeed, dopamine treatment profoundly diminished endogenous levels of both miR-1224 (14-fold, $p < 0.01$) (Fig. 8a) and miR-300 (20-fold, $p < 0.001$) (Fig. 8b) as compared to the control/untreated condition. ChIP assays revealed that the affinity of CREB to the MAO-B promoter is significantly enhanced upon dopamine treatment compared to control (1.8-fold, $p < 0.05$); however, there was no significant change in the binding of P-CREB to the MAO-B promoter following dopamine treatment (Fig. 8c). These results indicate the involvement of CREB in dopamine-mediated MAO-B gene expression.

To further assess the role of CREB in dopamine-mediated MAO-B gene expression, we transfected the MAO-B promoter construct into N2a cells followed by dopamine treatment. Dopamine caused a significant increase in the MAO-B promoter activity (2.2-fold, $p < 0.01$, Fig. 8d). Co-transfection of MAO-B promoter construct with KCREB decreased MAO-B promoter activity (5-fold, $p < 0.05$, Fig. 8d). Increase in MAO-B promoter activity mediated by dopamine was blocked

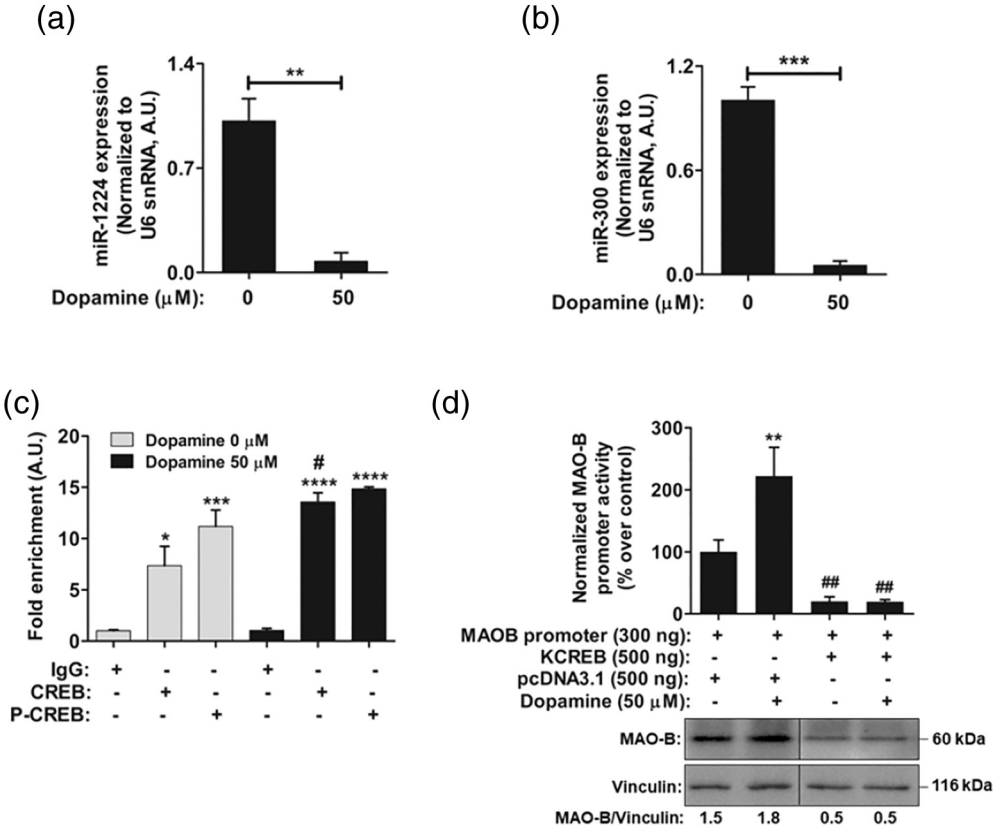

Fig. 8. Dopamine induces MAO-B by modulating endogenous miR-1224 and miR-300 levels and binding of CREB to the MAO-B promoter. Real-time PCR was performed following dopamine treatment using miR-1224 and U6 snRNA-specific primer (a) or with miR-300 and U6 snRNA-specific primer (b). Statistical significance was determined by Student's *t* test (unpaired, two-tailed). $^{**}p < 0.01$, $^{***}p < 0.001$ with respect to untreated/control. (c) ChIP assay was carried out with chromatin isolated from either control or dopamine-treated N2a cells using CREB, P-CREB, or IgG antibodies. Real-time PCR was performed with chromatin purified from respective cocktails using MAO-B gene-specific primer pair. Statistical significance was determined by one-way ANOVA with Bonferroni's multiple comparisons post-test. $^{*}p < 0.05$, $^{***}p < 0.001$, $^{****}p < 0.0001$ as compared to the corresponding IgG. $^{\#}p < 0.05$ as compared to CREB under basal condition (bar graph, second bar). (d) N2a cells transfected with MAO-B promoter–reporter construct in the presence or absence of KCREB were treated with dopamine. The promoter activities were normalized with total protein, and the results are expressed as percentage over control. The results are mean ± SE of triplicate values. Statistical significance was determined by one-way ANOVA with Bonferroni's multiple comparisons post-test. $^{**}p < 0.01$ with respect to basal MAO-B promoter activity. $^{\#\#}p < 0.01$ with respect to MAO-B plus dopamine (bar graph, second bar). Western blot displaying MAO-B protein in each case is shown. Relative levels of MAO-B after normalization with vinculin are shown.

by KCREB (11-fold, $p < 0.01$, Fig. 8d) suggesting the involvement of CREB under dopamine-induced condition. In addition to the promoter activity, the increase in endogenous MAO-B protein levels was also blunted upon KCREB transfection (lane 4, Fig. 8d). Taken together, these results underscore a regulatory role of CREB in dopamine-induced MAO-B expression.

Correlation between MAO-B levels and regulatory molecular factors in human tissues and rodent models of essential hypertension

Since the binding sites for Sp1, Egr1, and CREB are conserved across human, rat, and mouse, we next investigated if there is any correlation between the transcript levels of MAO-B and the factors involved in its regulation. For correlation analysis between the transcript levels of human MAO-B and Sp1/Egr1/CREB across various tissues, RNA-seq data from the GTEx portal (https://www.gtexportal.org/home/) were utilized (Table S10) [28]. Notably, there was a significant positive correlation between the transcript levels of MAO-B and Sp1 (Pearson $r = 0.35$, $p = 0.02$) (Fig. 9a), MAO-B and Egr1 (Pearson $r = 0.38$, $p = 0.01$) (Fig. 9b), and MAO-B and CREB (Pearson $r = 0.34$, $p = 0.03$) (Fig. 9c) across various tissues (n = 38), suggesting that these transcription factors could play important roles in regulating MAO-B gene expression. Such a correlation, however, was not observed between MAO-B and AP2alpha (Fig. S8).

Next, we estimated MAO-B levels in spontaneously hypertensive rat (SHR) *versus* normotensive Wistar Kyoto (WKY) rat tissues. Interestingly, the MAO-B mRNA level was lower (2.2-fold, $p < 0.05$) (Fig. 9d) in the brain tissues of SHR compared to WKY. Furthermore, mRNA levels of Sp1 and CREB were lower (2-fold, $p < 0.05$, and 1.6-fold, $p < 0.05$), while there was no significant difference in the mRNA level of Egr1 between SHR and WKY brain tissues. These results suggest that lower levels of Sp1 and CREB may account for lower MAO-B expression in SHR brain tissues. In the heart tissues, mRNA level of MAO-B was ~16-fold lower in SHR compared to WKY, but the difference did not reach statistical significance ($p = 0.11$) (Fig. 9d). However, the MAO-B protein level was significantly diminished in SHR compared to WKY (Figs. 9f and S6A). Moreover, the mRNA level of Sp1 was 4.6-fold ($p < 0.05$) lower in SHR compared to WKY, whereas the mRNA levels of Egr1 and CREB did not significantly differ between SHR and WKY (Fig. 9d).

We also quantified the mRNA level of MAO-B in a mouse model of human essential hypertension; MAO-B transcript level was higher in the BPL mouse liver when compared to BPH mouse (3.3-fold, $p < 0.05$) (Fig. 9e). Moreover, the protein level of MAO-B tends to be higher in BPL as compared to BPH mouse (Figs. 9g and S6B). Since our *in vitro* results suggest that miR-1224 and miR-300 regulate the expression of mouse MAO-B, we also quantified the levels of these miRNAs in BPH and BPL liver tissues. The level of miR-1224 was significantly higher in BPH liver tissue as compared to BPL liver tissue (2.6-fold, $p < 0.001$), whereas there was no significant difference in the miR-300 level (Fig. 9e), suggesting that increased level of miR-1224 might contribute to diminished MAO-B expression in BPH liver tissue.

Discussion

Monoamine oxidase inhibitors are routinely used to treat depression, PD, and other neurological disorders. Although it is well documented that the expression of MAO-B increases with age [7] and numerous reports strongly suggest that altered levels of MAO-B are associated with various pathological conditions including neurodegenerative diseases [10], metabolic disorders [19], and cardiac diseases [20], the molecular factors governing MAO-B gene regulation remain incompletely understood. Hence, in this study, we set out to identify the key motifs in the regulatory regions (i.e., the promoter and 3′-UTR) of MAO-B, transcription factors, and miRNAs that might regulate MAO-B gene expression both under basal and pathological conditions.

Transcription factors involved in regulating MAO-B gene expression

There are very few reports on regulation of MAO-B gene expression. Ethanol consumption in humans and rats leads to increase in MAO-B expression, which is mediated by GAPDH (glyceraldehyde 3-phosphate dehydrogenase) and TIEG-2 (transforming growth factor-beta-inducible early growth response protein 2) [21]. The transcription factors c-Jun and Egr1 play a key role in phorbol 12-myristate 13-acetate (PMA)-induced MAO-B activation [22]. Sp1 and Sp4 enhance human MAO-B expression, while Sp3 represses its expression [23,24]. Our stringent computational analysis and promoter/reporter assays suggest that the promoter domain (−144 to −78 bp) harboring putative binding sites for Sp1, Egr1, and CREB is crucial for MAO-B gene expression (Fig. 1). Consistently, over-expression/down-regulation of these factors (Sp1/Egr1/CREB) augmented/diminished the promoter–reporter activity and endogenous MAO-B protein levels (Fig. 2). In corroboration, mutations to abrogate the transcription factor binding sites (Fig. 3), EMSA and ChIP assays provided further evidence for *in vitro* and *in vivo* interaction of these transcription factors with the MAO-B promoter (Figs. 4 and 5). These findings suggest that Sp1, Egr1, and CREB regulate MAO-B gene expression under basal conditions. Of note, the binding sites for these transcription factors (Sp1, Egr1, and CREB) are conserved across the human, rat, and mouse MAO-B promoters (Fig. S1B). Consistently,

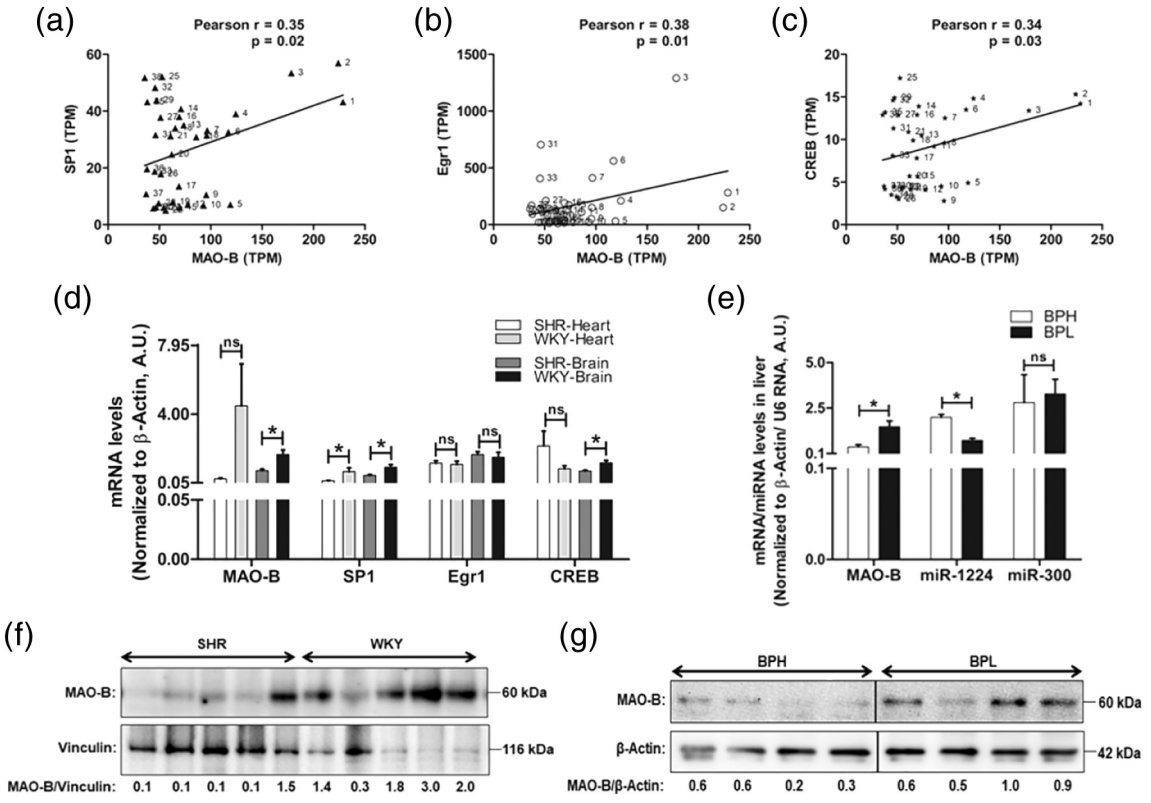

Fig. 9. MAO-B levels correlate with the regulatory molecular factors governing its expression in human tissues and rodent models of hypertension. Correlation between the transcript levels of MAO-B and Sp1 (a), MAO-B and Egr1 (b), and MAO-B and CREB (c) in various human tissue samples (n = 38; the identity of the tissue samples [indicated numerically in this figure] is given in the Supplemental Table S10) using data from GTEx portal. (d) The endogenous transcript levels of MAO-B, Sp1, Egr1, and CREB in the heart and brain tissues of SHR/WKY (n = 5) normalized with respect to β-actin. (e) The endogenous mRNA levels of MAO-B, microRNA levels of miR-1224, and miR-300 in the liver tissues of BPH/BPL (n = 4) normalized with respect to β-actin (for MAO-B) and U6 snRNA (for miR-1224 and miR-300). Western blot depicting the endogenous protein levels of MAO-B in the heart tissues from SHR and WKY rats (f) and in the liver tissues from BPH and BPL mice (g). Statistical significance was determined by Student's *t* test (unpaired, two-tailed). $^*p < 0.05$ with respect to corresponding SHR or BPH mRNA/miRNA levels (ns, not significant).

Sp1 and Egr1 have been previously reported to regulate human MAO-B gene expression [22]. Co-transfection of the human MAO-B promoter with CREB expression plasmid resulted in significant increase in the promoter activity (Fig. S7), suggesting a similar role for CREB in regulating human MAO-B gene expression.

Do these three transcription factors regulate MAO-B gene in a co-ordinated manner? Consistent with our computational prediction and previous reports for other genes [29,30], results of our co-transfection experiments (using equimolar amounts of the three transcription factors in various combinations) suggest that Sp1 and Egr1 compete with each other for binding to the MAO-B proximal promoter and that Sp1, Egr1, and CREB regulate MAO-B gene expression synergistically (Fig. S3).

Sp1 is also involved in regulating MAO-A expression (the index member of the monoamine oxidase family and a catecholamine-catabolizing enzyme) [31]. Notably, this study, for the first time, demonstrates an important role for CREB in regulating MAO-B gene expression. Interestingly, several genes responsible for catecholamine biosynthesis (i.e., tyrosine hydroxylase, dopamine beta-hydroxylase, phenylethanolamine *N*-methyltransferase) [32–38] and storage (*viz.*, chromogranin A and chromogranin B) [39,40] have also been reported to be regulated by Sp1, Egr1, and CREB. Taken together, these findings indicate vital roles of Sp1, Egr1, and CREB in modulating catecholamine homeostasis (biosynthesis/storage/catabolism).

Post-transcriptional regulation of MAO-B gene expression

miRNAs may play a crucial role in governing gene expression at the post-transcriptional level under pathophysiological conditions. However, there are no reports on the role of miRNAs in regulating MAO-B gene expression. Our stringent computational

analysis combined with experimental validation revealed roles for miR-1224 and miR-300 in MAO-B gene regulation. Of note, the levels of miR-1224 in mouse liver are augmented following ischemia/reperfusion (I/R) injury [41]. H_2O_2 produced as a by-product of MAO-B catalysis could potentially contribute to I/R injury, which is supported by the observations that MAO inhibitors offer protection against I/R injury [42] and against oxidative stress in rats [43]. A recent report indicated that Ang II/LPS-induced enhancement of MAO-A/MAO-B contributed to endothelial dysfunction in mouse [44]. Notably, LPS induces miR-1224 expression, which negatively regulates Sp1 [45]; miR-1224 also down-regulates CREB expression by binding to its 3′-UTR [46]. We speculate that the increase in miR-1224 could be a compensatory mechanism to suppress the deleterious effects of MAO-B expression under I/R injury. In addition, *in silico* analysis of the 3′-UTR of Egr1 revealed putative binding sites for miR-300. Perhaps, there could be cross-talks between the transcription factors (Sp1/Egr1/CREB) and miRNAs (miR-1224 and miR-300) in regulating MAO-B gene expression. Further studies are required for experimental validation of this speculation.

Dopamine-induced MAO-B gene expression: role of CREB, miRNA-1224 and miRNA-300

Dopamine is a substrate for MAO-B [3] and extracellular dopamine signals *via* the cAMP-PKA-CREB axis to modulate the expression of several genes [2]. Furthermore, MAO-B-dependent dopamine catabolism causes apoptosis in renal epithelial cells, which is prevented by MAO-B inhibitor [47]. In view of these reports, we sought to investigate the effect of dopamine on MAO-B expression and the potential mechanisms. Dopamine augmented the MAO-B promoter activity, and mRNA and protein levels (Fig. 7a, b, g, h). Moreover, forskolin and 8-Br-cAMP increased the promoter activity (Fig. 7c, d) and endogenous MAO-B protein levels (Fig. S5). Inhibition of PKA, on the other hand, attenuated the promoter activity and endogenous MAO-B protein levels (Fig. 7e, f), suggesting involvement of adenylate cyclase, cAMP and protein kinase A in MAO-B gene regulation. These results are in agreement with an increase in the MAO-B enzyme activity upon exposure to agents that augment intracellular cAMP levels [48]. MAO-B gene expression has also been reported to be enhanced by PKC and MAPK signaling pathways [22]. Moreover, CREB is a downstream target of PKC and MAPK [49]. Indeed, dopamine treatment significantly enhanced the binding of CREB to the MAO-B promoter and inhibition of CREB function profoundly diminished the dopamine-induced MOA-B expression (Fig. 8c, d). Thus, dopamine-induced MAO-B gene transcription is likely to involve multiple pathways.

Of note, this study, for the first time, revealed that dopamine caused a significant down-regulation in the endogenous miR-1224 and miR-300 levels (Fig. 8a, b). Our data suggest that there could be a feed-back loop between CREB and miR-1224/miR-300 under dopamine-stimulated MAO-B gene regulation. Interestingly, levodopa, a precursor of dopamine, is used for treatment of PD [50]; MAO-B inhibitors used in combination with levodopa appear to be more effective/beneficial than levodopa as a monotherapy [51,52]. These results offer molecular insights into the benefits of using MAO-B inhibitors as an adjunct to levodopa in PD management and prevention of apoptosis in renal epithelial cells.

Molecular basis for differential expression of MAO-B under pathophysiological conditions

Is there any correlation between the MAO-B levels and the factors involved in its regulation in different mammalian species and tissue types? To address this, we mined the transcriptomics data of MAO-B, Sp1, Egr1, and CREB from GTEx portal. As shown in (Fig. 9a–c), there was a significant positive correlation between the MAO-B transcript levels and the transcription factors across various tissues of human origin, suggesting that these transcription factors could regulate MAO-B expression in human tissues.

Based on previous reports that document diminished transcript levels of MAO-B in the adrenal gland [53] and heart tissues of SHR compared to WKY [54], we quantitated the transcript level of MAO-B in brain tissues from SHR and WKY. SHR is a routinely sought model for understanding pathological conditions such as essential human hypertension and attention-deficit hyperactivity disorder [55]. Consistent with previous reports, we found that the MAO-B transcript levels were lower in the heart tissue of SHR compared to WKY. A similar trend was also observed in the brain (Fig. 9d). Notably, the protein levels were also lower in the SHR heart compared to WKY (Fig. 9f). Could the transcription factor(s) involved in MAO-B regulation account for this observation? Indeed, the Sp1 mRNA level was significantly lower in the heart and brain tissues of SHR compared to WKY, suggesting lower levels of Sp1 could contribute to lower MAO-B transcript levels in SHR compared to WKY (Fig. 9d). In addition to the diminished expression of Sp1 in SHR brain, the transcript level of CREB was also significantly lower, which might account for, at least partly, the lower MAO-B expression in SHR brain (Fig. 9d).

A microarray analysis using various tissues from BPH/BPL mouse models revealed that the MAO-B mRNA levels were higher in liver and heart tissues of BPL compared to BPH mouse [Gene Expression Omnibus database (accession number GSE19817)] [56]. In view of this report and the observation that miR-1224 is expressed in mouse liver [41], we

estimated the levels of MAO-B and miRNAs in BPH/BPL liver. Indeed, in corroboration with the previous results, the transcript levels of MAO-B were significantly higher in the liver tissues of BPL compared to BPH (Fig. 9e). In addition, the protein levels of MAO-B were also higher in the BPL liver compared to BPH (Fig. 9g). In contrast, the miR-1224 levels are significantly lower in BPL (Fig. 9e), suggesting that lower levels of miR-1224 could contribute to higher MAO-B transcript levels in BPL mice. These results suggest roles of Sp1, CREB, and miR-1224 in regulating MAO-B gene expression in these rodent models of hypertension (BPH and SHR) wherein these molecular factors may diminish the MAO-B level, which in turn may result in elevated catecholamine levels (that can increase the blood pressure in these animals).

It is well known that MAO-B plays a central role in the conversion of neurotoxin MPTP to MPP^+ leading to dopaminergic neuronal cell death [57], which is prevented by administration of MAO-B inhibitors prior to MPTP injection [58]. In corroboration, MAO-B knockout mice are resistant to MPTP-induced neurotoxicity [9]. Strikingly, Sp1 is predicted to play a central role in MPTP toxicity [59] and the levels of Sp1 increase following MPP^+ treatment in PC12 and SH-SY5Y cells [60,61]. Moreover, Egr1 expression is also significantly up-regulated in MPTP mouse model and Egr1 knockout mice are resistant to the MPTP-induced loss of dopaminergic neurons [62]. Consistently, mithramycin A and its analogues, by interfering with the binding of Sp1 to the promoter and by inhibiting the transcriptional activity of Egr1, offer neuroprotection against MPTP [60,63]. Thus, the regulatory mechanisms of MAO-B expression, as per our data, are in agreement with these reports suggesting possible roles for these factors in neurodegenerative diseases (such as PD).

Conclusions and Perspectives

This systematic study identified the crucial *cis*-elements and transcription factors that govern MAO-B gene expression under basal and dopamine-induced conditions. It revealed the synergistic role for Sp1/Egr1/CREB in regulating MAO-B at the transcriptional level. The study also identified miR-1224 and miR-300 as novel regulators of MAO-B at the post-transcriptional level. A schematic presentation of our proposed mechanism of MAO-B regulation by these factors is presented in Fig. 10. Notably, the expression pattern of MAO-B and Sp1/Egr1/CREB corelated well in various human tissues. The molecular mechanisms of MAO-B regulation also might hold true under several cardiovascular (*viz.* in rodent models of human hypertension) and neuronal (*viz.* in MPTP-induced neurodegeneration) pathological conditions. The identified molecular regulators (including the miRNAs) may be targeted (after careful evaluation for off-target effects) for development of novel therapeutic agents in pathological conditions associated with dysregulated MAO-B expression.

Materials and Methods

Generation of mouse MAO-B promoter–reporter, MAOB-3′-UTR-reporter constructs, and microRNA expression plasmids

Varying lengths of MAO-B promoter (−1473, −1034, −346, −286, and −144 bp to +25 bp) regions were amplified using Blood Pressure Normal mouse genomic DNA (obtained from the Jackson Laboratory, USA) as template, Phusion® High-Fidelity DNA polymerase (Finnzymes, USA) and primers specific to the MAO-B promoter (NCBI reference number: NM_172778.2) (Table S1). PCR-amplified DNA segments were cloned at *Mlu*I and *Xho*I sites in the promoter-less firefly luciferase reporter vector pGL3-Basic (Promega, USA). These constructs were named as MAOB–pro-1473, MAOB–pro-1034, MAOB–pro-346, MAOB–pro-286, and MAOB–pro-144, respectively. MAOB–pro-695 and MAOB–pro-77 constructs were generated by digesting MAOB–pro-1473 construct with KpnI and SacI restriction enzymes, respectively, followed by gel purification and self-ligation of the larger fragment. Similarly, MAO-B 3′-UTR region was amplified using mouse genomic DNA as template, Phusion® High-Fidelity DNA polymerase and MAO-B 3′-UTR specific primer (Table S2). The resulting amplicon was cloned at XhoI and NotI sites in the pMIR-REPORT vector (Life technologies, USA). The mmu-miR-1224, mmu-miR-300, and mmu-miR-532 expression plasmids were generated by using mouse genomic DNA as template, Phusion® High-Fidelity DNA polymerase and primers to amplify regions flanking the pre-miRNA-1224, 300, and 532 sequences (Table S3). The PCR products were cloned at BamHI and XhoI sites in pcDNA3.1 vector (Invitrogen, USA). The sequence and orientation of all these DNA segments were confirmed by sequencing.

In silico analysis of mouse MAO-B core promoter and MAO-B 3′-UTR regions

The putative transcription factors binding sites in the MAO-B core promoter (*viz.*, −144- to +1-bp region, which gave the highest reporter activity) were identified using three transcription factor prediction tools (as mentioned in Table S4). Various miRNA binding site prediction tools (as mentioned with Table S5) were used to predict the putative miRNAs that might interact with the MAO-B 3′-UTR similar to

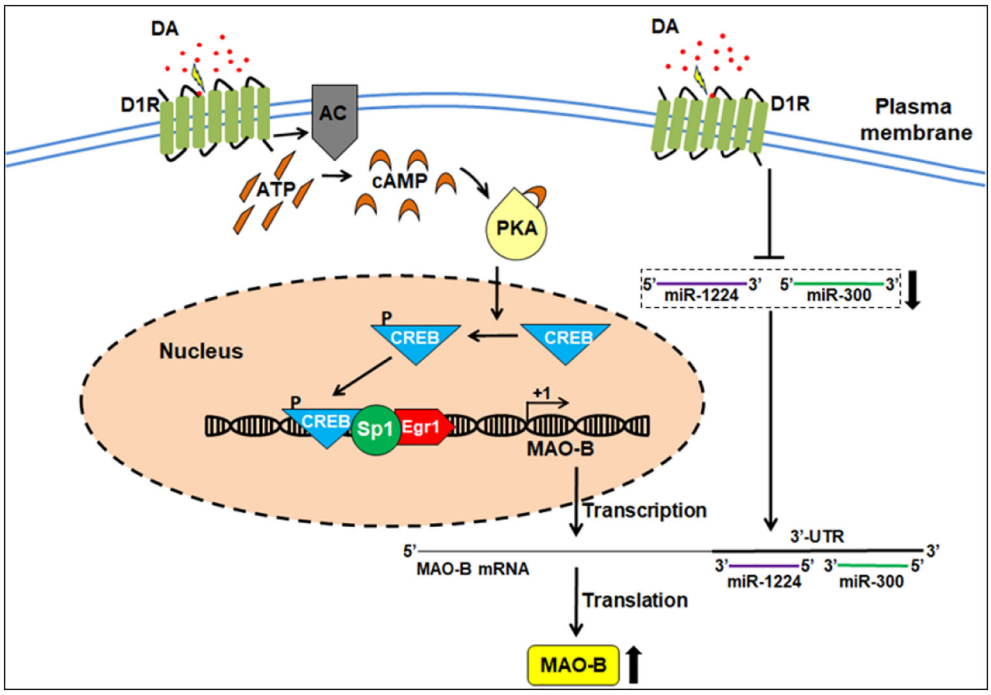

Fig. 10. Plausible mechanisms modulating MAO-B gene expression under basal and dopamine-induced conditions. While the transcription factors Sp1, Egr1, and CREB regulate MAO-B gene expression at the transcriptional level, miRNAs —miR-1224 and miR-300—are involved at the post-transcriptional level. Dopamine-induced MAO-B expression is mediated by (a) enhanced binding of CREB to the MAO-B promoter, and (b) down-regulation of endogenous miR-1224/miR-300 and consequent diminished interactions at the MAO-B 3′-UTR. DA, dopamine; D1R, dopamine receptor D1; AC, adenylate cyclase. Up-regulation and down-regulation of MAO-B and miRNAs are shown by upward and blunted arrows, respectively.

our previously described approach in the case of renalase gene [64]. These *in silico* analysis revealed putative binding sites for several transcription factors and miRNAs. Transcription factors predicted by at least two programs and miRNAs predicted by at least four programs were short-listed (Tables S4 and S5, respectively) for experimental validation.

Cell culture, transfection, and reporter assays

Authenticated HEK-293, N2a, AGS, CHO, AML 12, and IMR-32 cell lines were obtained from the Indian national repository for cell lines and hybridomas at the National Center for Cell Sciences, Pune, India. Cells were cultured in Dulbecco's modified Eagle's medium with high glucose and glutamine (HyClone, USA), supplemented with 10% fetal bovine serum (Invitrogen, USA), penicillin G (100 U/mL), and streptomycin sulfate (100 mg/mL) (Invitrogen, USA) in 25-cm^2 tissue culture flasks (Nalgene-Nunc International, USA) at 37 °C with 5% CO_2 as described previously [65]. These cell lines were routinely tested for mycoplasma infection and treated with BM-Cyclin (Merck, USA) to eliminate mycoplasma, if detected. Transient transfections of the MAO-B promoter-reporter constructs (500 ng/well) were carried out in these cell lines by calcium-phosphate method [66]. A β-galactosidase expression plasmid (125 ng/well) was co-transfected as an internal control for transfection efficiency [67]. In some experiments, the MAO-B core promoter-reporter construct (*viz.*, MAOB–pro-144; 500 ng/well) was co-transfected with increasing doses (0, 125, 250, and 500 ng/well) of Sp1 expression plasmid (containing the human full-length Sp1 cDNA fused to the CMV promoter) or Egr1 expression plasmid (pCMV-Egr1 containing the entire human Egr1 cDNA under the control of CMV promoter obtained from Dr. Dona Lee Wong, Harvard Medical School, Boston) [68] or CREB expression plasmid (CREB-VP16, which contains basic-leucine zipper domain of CREB, and the transcriptional activation domain of the herpes virus VP16 protein was obtained from Dr. David Ginty, Howard Hughes Medical Institute) [69] or with Sp1-shRNA plasmid (obtained from Dr. Guido Marcucci, Ohio State University, Ohio) [70] or Egr1-shRNA plasmid (obtained from Dr. Weihua Xiao, University of Science and Technology of China, Hefei) [71] or KCREB (a dominant repressor of CREB, which has a single mutation, Arg → Leu, in the DNA binding domain compared to wild-type was obtained from Dr. Richard H. Goodman, Oregon Health Sciences University, Portland) [72] into N2a cells. Similarly, the MAO-B

core promoter construct (250 ng/well) was co-transfected with 250 ng of various combinations of Sp1, Egr1, and CREB expression plasmids. Likewise, the MAO-B core promoter-reporter construct (500 ng/well) was co-transfected with 5 nM of either control siRNA or CREB siRNA. In another set of experiments, N2a cells were transfected with the MAO-B core promoter-reporter construct (300 or 500 ng/well); following 12 h post-transfection, cells were treated with 8-Br-cAMP (0, 1, 2.5, and 5 μM) or forskolin (0, 1, 5, and 10 μM) or dopamine (0, 5, 10, 20, 25, and 50 μM). To check the time-dependent effect of dopamine on the promoter activity, N2a cells transfected with the MAO-B core promoter-reporter construct were treated with 50 μM dopamine for different time points (0, 3, 6, 9, and 12 h). Cells treated with 8-Br-cAMP/forskolin and dopamine were lysed 24 and 12 h post-treatment, respectively, for luciferase and Bradford's assays (for total protein estimation). In order to assess the effect of inhibiting PKA on the MAO-B promoter activity, N2a cells were co-transfected with MAO-B promoter-reporter construct (500 ng/well) and increasing doses (0, 125, 250, 500, and 1000 ng/well) of PKI expression plasmid [pRSV-PKI-v2 generated by Dr. Richard Maurer was obtained from Addgene (Plasmid No. 45066)]. Similarly, MAOB–3′UTR reporter construct (500 ng/well) was co-transfected with increasing concentrations (0, 250, 500, and 1000 ng/well) of miR-1224, miR-300, or miR-532 expression plasmids and pMIR-Report beta-gal control vector (125 ng/well) (Life technologies, USA). For all the co-transfection experiments, following 24 h of transfection, cells were lysed for luciferase and either beta-gal assays or total protein estimation as described previously [67]. In all these experiments, the reporter activities were either normalized to β-galactosidase activity or total protein, and the results are expressed as percentage fold change over basal.

Generation of mutations in the putative transcription factor binding sites in mouse MAO-B promoter

Mutations were generated at the Sp1/Egr1 and CREB binding sites by site-directed mutagenesis using wild-type promoter–reporter plasmid as template and a primer pair with the desired mutation (Table S6). The resulting plasmids were named MAOB–pro-Sp1/Egr1-mut and MAOB–pro-CREB-mut. Next, N2a cells were co-transfected with either the wild-type or MAOB–pro-Sp1/Egr1-mut promoter-reporter constructs (500 ng/well) and increasing doses (0, 125, 250, and 500 ng/well) of either Sp1 or Egr1 expression plasmids. Similarly, N2a cells were also co-transfected with either the wild-type or MAOB–pro-CREB-mutant promoter-reporter constructs (500 ng/well) and increasing doses (0, 125, 250, and 500 ng/well) of CREB expression plasmid. Cells were lysed 24 h after transfection and assayed for luciferase activity. The protein contents were measured in cell lysates using Bradford's assay reagent (Bio-Rad, USA). Luciferase activities in cell lysates were normalized with total protein, and the results were expressed as percentage over control.

Western blotting for MAO-B, Sp1, Egr1, and CREB protein levels in N2a cells and rodent tissues

In order to confirm the over-expression or down-regulation of transcription factors and their effect on endogenous levels of MAO-B, N2a cells (seeded in 6-well plates) were co-transfected with MAO-B promoter-reporter construct (500 ng/well) and increasing doses (0, 125, 250, and 500 ng/well) of Sp1 or Egr1 or CREB expression plasmids or with increasing doses (0, 125, 250, and 500 ng/well) of Sp1-shRNA or Egr1-shRNA expression plasmid or KCREB plasmid using Targefect F2 transfection reagent (Targeting Systems, USA). N2a cells were also co-transfected with MAO-B promoter-reporter construct and with either 5 nM control or CREB siRNA (Integrated DNA Technologies, Belgium). Similarly, to ascertain the effect of over-expression of miRNAs on the endogenous levels of MAO-B, MAOB–3′UTR reporter construct (500 ng/well) was co-transfected with increasing concentrations (0, 250, 500, and 1000 ng/well) of miR-1224 or miR-300 expression plasmids using Targefect F2 transfection reagent. In another set of experiments, 50 nM of control oligo, miR-1224, and miR-300 mimics or inhibitors (Exiqon, Denmark) were transfected into N2a cells using Targefect F2 transfection reagent. To check the effect of inhibiting PKA on endogenous MAO-B levels, N2a cells (seeded in 6-well plates) were co-transfected with MAO-B promoter-reporter construct (500 ng/well) and increasing doses (0, 500, and 1000 ng/well) of PKI expression plasmid using Targefect F2 transfection reagent. In each case, following 24 h post-transfection, cells were lysed in RIPA buffer [50 mM Tris–HCl (pH 7.2), 150 mM NaCl, 1% (v/v) Triton X-100, 1% (w/*v*) sodium deoxycholate and 0.1% (w/v) SDS] with PMSF and protease inhibitor cocktail (Sigma, USA) for Western blot analysis. Total protein was also isolated from N2a cells transfected with MAO-B promoter-reporter construct (500 ng/well) and treated with dopamine (0 to 50 μM) for 12 h and forskolin (1, 5, and 10 μM) or 8-Br-cAMP (2.5 μM) for 24 h. Similarly, total proteins were isolated from heart tissues of SHR/WKY rats and liver tissues of BPH/BPL mice. Protein concentrations in the cell lysates were estimated using Bradford assay (Bio-Rad). About 30–40 μg of proteins was separated on a 10% SDS-polyacrylamide gel and transferred to a PVDF membrane (Pall Life Sciences, Mexico). Pre-stained protein ladder (Abcam) was used as a molecular marker. After blocking with 3% of BSA or 5% of non-fat milk for 1 h at room temperature, the membranes were incubated with specific primary antibody [Sp1 (Santa Cruz Biotechnologies, sc-59x) at 1:3000 dilution, Egr1 (Cell Signaling Technology, No. 4153) at 1:1500

dilution, CREB (Santa Cruz Biotechnologies, sc-186x) at 1:3000 dilution, MAO-B (Santa Cruz Biotechnologies, sc-18401) at 1:5000 dilution, Vinculin (Sigma, V9131) at 1:7500 dilution, and β-Actin (Sigma, A5441) at 1:10000 dilution] overnight at 4 °C. After washing with 1× TBST, the membrane was incubated with HRP-conjugated secondary antibody specific for either rabbit (Jackson Immunoresearch No. 111-035-003 at 1:5000 dilutions for detection of Sp1, Egr1, and CREB) or mouse (Jackson Immunoresearch No. 115-035-003 at 1:5000 dilution for detection of Vinculin and β-Actin) or goat (Abcam, ab6741 at 1:5000 dilution for detection of MAO-B) for 1 h. The protein bands were detected using chemiluminescent ECL Detection System (Pierce, USA). The intensities of bands were quantified using NIH Image Lab 3.0.

Electrophoretic mobility shift assays

Nuclear protein extracts from N2a cells and N2a cells transfected with either Sp1 or Egr1 expression plasmid were prepared using nuclear protein extraction kit (Thermo-scientific, USA) as described by the manufacturer and stored in aliquots at −80 °C until use. Wild-type (harboring binding sites for specific transcription factors), mutant (harboring mutations at the binding sites for specific transcription factors), or CREB binding site deleted oligos and their complementary strands were synthesized by Bioserve Technologies, India (Table S7). The single-stranded oligomers were biotinylated using the Biotin 3′-End Labeling Kit (Pierce, USA) and annealed. For EMSA, 10 µg of nuclear protein extract was incubated with the binding buffer (10 mM Tris, 50 mM KCl, and 1 mM dithiothreitol at pH 7.5), 50 ng/µl poly-dI-dC, and 25 fmol of biotinylated oligo as described previously [67]. For competitive EMSA, increasing amounts of unlabeled wild-type/mutant oligos were added 1 h prior to the addition of the constant amount of the labeled wild-type oligos into the reaction mixture. In some EMSA experiments, specific antibodies against Sp1 (Santa Cruz Biotechnologies, sc-59x), Egr1 (Cell Signaling Technology, No. 4153), CREB (Santa Cruz Biotechnologies, sc-186x), and rabbit pre-immune IgG antibody (I5006, Sigma) were added 1 h prior to the addition of labeled oligos. The reaction mixtures were resolved on 1.5-mm-thick 5% non-denaturing polyacrylamide gels and transferred to Hybond-N+ membranes (Amersham, USA). The complexes were UV cross-linked to the membrane and the labeled probes were detected using the LightShift Chemiluminescent EMSA Kit (Pierce, USA).

ChIP assays

ChIP assays were carried out as described earlier [67]. In brief, exponentially growing N2a cells were cross-linked using 1% formaldehyde, lysed, and nuclei pellets were collected by centrifugation and re-suspended in nuclei lysis buffer. Sonication was carried out to fragment the chromatin, and sheared chromatin was used for subsequent immunoprecipitation. Pre-cleared chromatin supernatants were subjected to immunoprecipitation at 4 °C overnight using 4 µg ChIP-grade antibodies against Sp1 (Santa Cruz Biotechnologies, sc-59x) or CREB (Santa Cruz Biotechnologies, sc-186x), or Egr1 (Cell Signaling Technology, No. 4153), in 1× ChIP buffer supplemented with protease inhibitor cocktail. As a negative control, an equal amount of chromatin was precipitated with rabbit pre-immune IgG antibody (I5006, Sigma). Specific antibody–chromatin complexes were then precipitated by incubation with ChIP-grade protein-G-coated Sepharose beads (Invitrogen, USA) for 4 h at 4 °C. DNA samples were eluted, and supernatants were used for reverse cross-linking protein/DNA complexes to free DNA. The purified DNA was subjected to PCR amplification using specific primer pair encompassing the transcription factor binding domain or a primer pair outside this domain that served as a control (Table S8).

In another set of experiments, chromatin was isolated from N2a cells with or without 50 µM dopamine exposure. Immunoprecipitation of chromatin fragments was carried out using ChIP-grade antibodies against CREB (Santa Cruz Biotechnologies, sc-186x) and P-CREB (No. 9198, Cell Signaling Technology, USA). Pre-immune IgG was used as a negative control. Enrichment of the MAO-B promoter domains in the immunoprecipitated chromatin from basal or dopamine induced condition was determined by real-time PCR using DyNAmo™ Flash SYBR Green qPCR Kit (No. F416 L, Finnzymes, USA) and specific primers (Table S8). Data were represented as fold change over IgG antibody.

Mouse and rat strains and tissue samples

Liver tissue samples from 5- to 7-week-old male BPH (Blood Pressure High strain BPH/2J at inbred generation F66, n = 4) and BPL (Blood Pressure Low strain BPL/1J at inbred generation F65, n = 4) mouse models of essential hypertension were obtained from Jackson Laboratory, USA. Brain and heart tissues were harvested from 4- to 6-week-old male SHR (n = 5) and normotensive control rats WKY (n = 5). To minimize the effect of age-related confounding factors on gene expression, rodents of early age were selected for this study. The animal experiments were approved by Institute Animal Ethics Committee of IIT Madras.

RNA isolation and quantitative real-time PCR

Total RNA was isolated from N2a cells with or without dopamine treatment using Trizol (Invitrogen, USA). cDNA was synthesized using 2 µg RNA, random

hexamers and High Capacity cDNA Reverse Transcription Kit (Applied Biosystems, USA). Similarly, total RNA was isolated from mouse/rat tissue samples using TRIzol and NucleoSpin miRNA kit (Macherey-Nagel, USA) and were subjected to cDNA synthesis. In order to determine the mRNA levels, quantitative real-time PCR (qPCR) was carried out using DyNAmo™ Flash SYBR Green qPCR Kit and MAO-B, Sp1, Egr1, and CREB transcript-specific primer pairs (Table S9). The mRNA levels of β-actin were quantified for normalization of gene expression using actin-specific primer pair (Table S9).

In order to quantify the miRNA levels, total RNA was isolated from liver tissues of BPH and BPL mice using TRIzol and NucleoSpin miRNA kit. Total RNA was also isolated from N2a cells with or without exposure to 50 μM dopamine for 12 h using TRIzol. Two micrograms of RNA sample was used to synthesize cDNA using high-capacity cDNA synthesis kit, miR-1224/miR-300 and U6-specific stem–loop reverse transcription primers (Table S9). qPCR was carried out using DyNAmo™ Flash SYBR Green qPCR Kit, miR-1224/miR-300 and U6 forward primers, and universal reverse primer (Table S9). The relative abundance in each sample was determined by calculating $2^{(-\Delta\Delta Ct)}$ as described previously [65].

Statistical analysis

For MAO-B promoter or 3′-UTR-reporter transient transfections, co-transfection experiments were carried out at least three times, and results were expressed as mean ± SEM of triplicates from representative experiments. Statistical significance was determined by Student's *t* test (unpaired, two-tailed) and one-way ANOVA with Bonferroni's multiple comparisons post-test, as appropriate, by using the Prism 5 program (GraphPad Software, USA).

Acknowledgments

This work was supported by a grant from the Department of Biotechnology, Government of India to NRM (project number: BT/PR5017/MED/30/756/2012). Research fellowships were received from the Department of Science and Technology (to V.A.), Ministry of Human Resource Development (to V.G., A.A., and A.A.K.), Council of Scientific and Industrial Research (to A.K. and B.N.), and Indian Council of Medical Research (to S.S.R.), Government of India. The authors are grateful to Dr. David Ginty (Howard Hughes Medical Institute) for the CREB-VP16 plasmid; to Richard H. Goodman (Vollum Institute, Oregon Health Sciences University, Portland), for the KCREB plasmid; to Dr. Dona Lee Wong (Harvard Medical School, Boston) for providing us with the Sp1 and Egr1 expression plasmids; to Dr. Guido Marcucci (Comprehensive Cancer Center, Ohio State University, Ohio) for the Sp1-shRNA plasmid; and to Dr. Weihua Xiao (University of Science and Technology of China, Hefei) for the Egr1-shRNA plasmid.

Appendix A. Supplementary data

Supplementary data to this article can be found online at https://doi.org/10.1016/j.jmb.2019.01.042.

Received 29 October 2018;
Received in revised form 18 January 2019;
Accepted 29 January 2019
Available online 7 February 2019

Keywords:
transcriptional regulation;
post-transcriptional regulation;
dopamine;
cyclic AMP;
protein kinase A

Abbreviations used:
MAO-B, monoamine oxidase B; Sp1, specificity protein 1; Egr1, early growth response 1; CREB, cAMP response element binding protein; DA, dopamine; cAMP, cyclic adenosine monophosphate; PKA, protein kinase A; ChIP, chromatin immunoprecipitation; EMSA, electrophoretic mobility shift assay; shRNA, short hairpin RNA; siRNA, small interfering RNA; 3′-UTR, 3′-untranslated region; miR, microRNA; MPTP, 1-methyl-4-phenyl-1,2,3,6-tetrahydropyridine; bp, base pair.

References

[1] M. Bortolato, G. Floris, J.C. Shih, From aggression to autism: new perspectives on the behavioral sequelae of monoamine oxidase deficiency, J. Neural Transm. (2018), https://doi.org/10.1007/s00702-018-1888-y.
[2] C. Rangel-Barajas, I. Coronel, B. Floran, Dopamine receptors and neurodegeneration, Aging Dis. 6 (2015) 349–368.
[3] H.L. White, A.T. Glassman, Multiple binding sites of human brain and liver monoamine oxidase: substrate specificities, selective inhibitions, and attempts to separate enzyme forms, J. Neurochem. 29 (1977) 987–997.
[4] S. Jo, O. Yarishkin, Y.J. Hwang, Y.E. Chun, M. Park, D.H. Woo, J.Y. Bae, T. Kim, J. Lee, H. Chun, H.J. Park, D.Y. Lee, J. Hong, H.Y. Kim, S.J. Oh, S.J. Park, H. Lee, B.E. Yoon, Y. Kim, Y. Jeong, I. Shim, Y.C. Bae, J. Cho, N.W. Kowall, H. Ryu, E. Hwang, D. Kim, C.J. Lee, GABA from reactive astrocytes impairs memory in mouse models of Alzheimer's disease, Nat. Med. 20 (2014) 886–896.
[5] B.E. Yoon, J. Woo, Y.E. Chun, H. Chun, S. Jo, J.Y. Bae, H. An, J.O. Min, S.J. Oh, K.S. Han, H.Y. Kim, T. Kim, Y.S. Kim, Y.C. Bae, C.J. Lee, Glial GABA, synthesized by monoamine oxidase B, mediates tonic inhibition, J. Physiol. 592 (2014) 4951–4968.

[6] Y. Arai, H. Kinemuchi, Differences between monoamine-oxidase concentrations in striatum and forebrain of aged and young-rats, J. Neural Transm. 72 (1988) 99–105.
[7] J.S. Fowler, N.D. Volkow, G.J. Wang, J. Logan, N. Pappas, C. Shea, R. MacGregor, Age-related increases in brain monoamine oxidase B in living healthy human subjects, Neurobiol. Aging 18 (1997) 431–435.
[8] D.A. Rothmond, C.S. Weickert, M.J. Webster, Developmental changes in human dopamine neurotransmission: cortical receptors and terminators, BMC Neurosci. 13 (2012) 18.
[9] J. Grimsby, M. Toth, K. Chen, T. Kumazawa, L. Klaidman, J.D. Adams, F. Karoum, J. Gal, J.C. Shih, Increased stress response and beta-phenylethylamine in MAOB-deficient mice, Nat. Genet. 17 (1997) 206–210.
[10] C.M. Woodard, B.A. Campos, S.H. Kuo, M.J. Nirenberg, M.W. Nestor, M. Zimmer, E.V. Mosharov, D. Sulzer, H.Y. Zhou, D. Paull, L. Clark, E.E. Schadt, S.P. Sardi, L. Rubin, K. Eggan, M. Brock, S. Lipnick, M. Rao, S. Chang, A.Q. Li, S.A. Noggle, iPSC-derived dopamine neurons reveal differences between monozygotic twins discordant for Parkinson's disease, Cell Rep. 9 (2014) 1173–1182.
[11] S. Schedin-Weiss, M. Inoue, L. Hromadkova, Y. Teranishi, N.G. Yamamoto, B. Wiehager, N. Bogdanovic, B. Winblad, A. Sandebring-Matton, S. Frykman, L.O. Tjernberg, Monoamine oxidase B is elevated in Alzheimer disease neurons, is associated with gamma-secretase and regulates neuronal amyloid beta-peptide levels, Alzheimers Res. Ther. 9 (2017) 57.
[12] J. Tong, G. Rathitharan, J.H. Meyer, Y. Furukawa, L.C. Ang, I. Boileau, M. Guttman, O. Hornykiewicz, S.J. Kish, Brain monoamine oxidase B and A in human parkinsonian dopamine deficiency disorders, Brain 140 (2017) 2460–2474.
[13] J.S. Fowler, J. Logan, G.J. Wang, N.D. Volkow, F. Telang, W. Zhu, D. Franceschi, N. Pappas, R. Ferrieri, C. Shea, V. Garza, Y. Xu, D. Schlyer, S.J. Gatley, Y.S. Ding, D. Alexoff, D. Warner, N. Netusil, P. Carter, M. Jayne, P. King, P. Vaska, Low monoamine oxidase B in peripheral organs in smokers, Proc. Natl. Acad. Sci. U. S. A. 100 (2003) 11600–11605.
[14] J.K. Mallajosyula, D. Kaur, S.J. Chinta, S. Rajagopalan, A. Rane, D.G. Nicholls, D.A. Di Monte, H. Macarthur, J.K. Andersen, MAO-B elevation in mouse brain astrocytes results in Parkinson's pathology, PLoS One 3 (2008), e1616.
[15] K. Chiba, A. Trevor, N. Castagnoli Jr., Metabolism of the neurotoxic tertiary amine, MPTP, by brain monoamine oxidase, Biochem. Biophys. Res. Commun. 120 (1984) 574–578.
[16] G. Cohen, P. Pasik, B. Cohen, A. Leist, C. Mytilineou, M.D. Yahr, Pargyline and deprenyl prevent the neurotoxicity of 1-methyl-4-phenyl-1,2,3,6-tetrahydropyridine (MPTP) in monkeys, Eur. J. Pharmacol. 106 (1984) 209–210.
[17] J. Knoll, The pharmacological basis of the beneficial effects of (–)deprenyl (selegiline) in Parkinson's and Alzheimer's diseases, J. Neural Transm. Suppl. 40 (1993) 69–91.
[18] L.R. Cataldo, M.L. Mizgier, D. Busso, P. Olmos, J.E. Galgani, R. Valenzuela, D. Mezzano, E. Aranda, V.A. Cortes, J.L. Santos, Serotonin- and dopamine-related gene expression in db/db mice islets and in MIN6 beta-cells treated with palmitate and oleate, J. Diabetes Res. 2016 (2016) 3793781.
[19] E. Ganic, J.K. Johansson, H. Bennet, M. Fex, I. Artner, Islet-specific monoamine oxidase A and B expression depends on MafA transcriptional activity and is compromised in type 2 diabetes, Biochem. Biophys. Res. Commun. 468 (2015) 629–635.
[20] N. Kaludercic, A. Carpi, T. Nagayama, V. Sivakumaran, G. Zhu, E.W. Lai, D. Bedja, A. De Mario, K. Chen, K.L. Gabrielson, M.L. Lindsey, K. Pacak, E. Takimoto, J.C. Shih, D.A. Kass, F. Di Lisa, N. Paolocci, Monoamine oxidase B prompts mitochondrial and cardiac dysfunction in pressure overloaded hearts, Antioxid. Redox Signal. 20 (2014) 267–280.
[21] X.M. Ou, C.A. Stockmeier, H.Y. Meltzer, J.C. Overholser, G.J. Jurjus, L. Dieter, K. Chen, D. Lu, C. Johnson, M.B. Youdim, M.C. Austin, J. Luo, A. Sawa, W. May, J.C. Shih, A novel role for glyceraldehyde-3-phosphate dehydrogenase and monoamine oxidase B cascade in ethanol-induced cellular damage, Biol. Psychiatry 67 (2010) 855–863.
[22] W.K. Wong, X.M. Ou, K. Chen, J.C. Shih, Activation of human monoamine oxidase B gene expression by a protein kinase C MAPK signal transduction pathway involves c-Jun and Egr-1, J. Biol. Chem. 277 (2002) 22222–22230.
[23] S.Y.A. Tsai, J.Y. Chuang, M.S. Tsai, X.F. Wang, Z.X. Xi, J.J. Hung, W.C. Chang, A. Bonci, T.P. Su, Sigma-1 receptor mediates cocaine-induced transcriptional regulation by recruiting chromatin-remodeling factors at the nuclear envelope, Proc. Natl. Acad. Sci. U. S. A. 112 (2015) E6562–E6570.
[24] W.K. Wong, K. Chen, J.C. Shih, Regulation of human monoamine oxidase B gene by Sp1 and Sp3, Mol. Pharmacol. 59 (2001) 852–859.
[25] S.P.R. Romaine, M. Tomaszewski, G. Condorelli, N.J. Samani, MicroRNAs in cardiovascular disease: an introduction for clinicians, Heart 101 (2015) 921–928.
[26] S.M. Eacker, T.M. Dawson, V.L. Dawson, Understanding microRNAs in neurodegeneration, Nat. Rev. Neurosci. 10 (2009) 837–841.
[27] K.B. Seamon, W. Padgett, J.W. Daly, Forskolin: unique diterpene activator of adenylate cyclase in membranes and in intact cells, Proc. Natl. Acad. Sci. U. S. A. 78 (1981) 3363–3367.
[28] G.T. Consortium, The genotype-tissue expression (GTEx) project, Nat. Genet. 45 (2013) 580–585.
[29] R.P. Huang, Y. Fan, Z.Y. Ni, D. Mercola, E.D. Adamson, Reciprocal modulation between Sp1 and Egr-1, J. Cell. Biochem. 66 (1997) 489–499.
[30] L.M. Khachigian, A.J. Williams, T. Collins, Interplay of Sp1 and Egr-1 in the proximal platelet-derived growth factor A-chain promoter in cultured vascular endothelial cells, J. Biol. Chem. 270 (1995) 27679–27686.
[31] V. Gupta, A.A. Khan, B.K. Sasi, N.R. Mahapatra, Molecular mechanism of monoamine oxidase A gene regulation under inflammation and ischemia-like conditions: key roles of the transcription factors GATA2, Sp1 and TBP, J. Neurochem. 134 (2015) 21–38.
[32] L. Aurelian, K.T. Warnock, I. Balan, A. Puche, H. June, TLR4 signaling in VTA dopaminergic neurons regulates impulsivity through tyrosine hydroxylase modulation, Transl. Psychiatry 6 (2016) e815.
[33] S.Y. Cheng, L.I. Serova, D. Glazkova, E.L. Sabban, Regulation of rat dopamine beta-hydroxylase gene transcription by early growth response gene 1 (Egr1), Brain Res. 1193 (2008) 1–11.
[34] S.N. Ebert, S.L. Balt, J.P. Hunter, A. Gashler, V. Sukhatme, D.L. Wong, Egr-1 activation of rat adrenal phenylethanolamine *N*-methyltransferase gene, J. Biol. Chem. 269 (1994) 20885–20898.
[35] S. Her, R. Claycomb, T.C. Tai, D.L. Wong, Regulation of the rat phenylethanolamine *N*-methyltransferase gene by transcription factors Sp1 and MAZ, Mol. Pharmacol. 64 (2003) 1180–1188.
[36] H.S. Kim, H. Seo, C.Y. Yang, J.F. Brunet, K.S. Kim, Noradrenergic-specific transcription of the dopamine beta-hydroxylase gene requires synergy of multiple cis-acting

elements including at least two Phox2a-binding sites, J. Neurosci. 18 (1998) 8247–8260.
[37] N.A. Papanikolaou, E.L. Sabban, Sp1/Egr1 motif: a new candidate in the regulation of rat tyrosine hydroxylase gene transcription by immobilization stress, J. Neurochem. 73 (1999) 433–436.
[38] T.C. Tai, K. Morita, D.L. Wong, Role of Egr-1 in cAMP-dependent protein kinase regulation of the phenylethanolamine *N*-methyltransferase gene, J. Neurochem. 76 (2001) 1851–1859.
[39] N.R. Mahapatra, M. Mahata, S. Ghosh, J.R. Gayen, D.T. O'Connor, S.K. Mahata, Molecular basis of neuroendocrine cell type-specific expression of the chromogranin B gene: crucial role of the transcription factors CREB, AP-2, Egr-1 and Sp1, J. Neurochem. 99 (2006) 119–133.
[40] R. Raychowdhury, G. Schafer, J. Fleming, S. Rosewicz, B. Wiedenmann, T.C. Wang, M. Hocker, Interaction of early growth response protein 1 (Egr-1), specificity protein 1 (Sp1), and cyclic adenosine 3′5′-monophosphate response element binding protein (CREB) at a proximal response element is critical for gastrin-dependent activation of the chromogranin A promoter, Mol. Endocrinol. 16 (2002) 2802–2818.
[41] S. Roy, H. Bantel, F. Wandrer, A.T. Schneider, J. Gautheron, M. Vucur, F. Tacke, C. Trautwein, T. Luedde, C. Roderburg, miR-1224 inhibits cell proliferation in acute liver failure by targeting the antiapoptotic gene Nfib, J. Hepatol. 67 (2017) 966–978.
[42] P. Bianchi, O. Kunduzova, E. Masini, C. Cambon, D. Bani, L. Raimondi, M.H. Seguelas, S. Nistri, W. Colucci, N. Leducq, A. Parini, Oxidative stress by monoamine oxidase mediates receptor-independent cardiomyocyte apoptosis by serotonin and postischemic myocardial injury, Circulation 112 (2005) 3297–3305.
[43] C. Ratiu, D. Utu, A. Petrus, P. Norbert, S. Olariu, O. Duicu, A. Sturza, D.M. Muntean, Monoamine oxidase inhibition improves vascular function and reduces oxidative stress in rats with lipopolysaccharide-induced inflammation, Gen. Physiol. Biophys. (2018), https://doi.org/10.4149/gpb_2018014.
[44] A. Sturza, M.S. Leisegang, A. Babelova, K. Schroder, S. Benkhoff, A.E. Loot, I. Fleming, R. Schulz, D.M. Muntean, R.P. Brandes, Monoamine oxidases are mediators of endothelial dysfunction in the mouse aorta, Hypertension 62 (2013) 140–146.
[45] Y. Niu, D. Mo, L. Qin, C. Wang, A. Li, X. Zhao, X. Wang, S. Xiao, Q. Wang, Y. Xie, Z. He, P. Cong, Y. Chen, Lipopolysaccharide-induced miR-1224 negatively regulates tumour necrosis factor-alpha gene expression by modulating Sp1, Immunology 133 (2011) 8–20.
[46] J. Qian, R. Li, Y.Y. Wang, Y. Shi, W.K. Luan, T. Tao, J.X. Zhang, Y.C. Xu, Y.P. You, MiR-1224-5p acts as a tumor suppressor by targeting CREB1 in malignant gliomas, Mol. Cell. Biochem. 403 (2015) 33–41.
[47] P. Bianchi, M.H. Seguelas, A. Parini, C. Cambon, Activation of pro-apoptotic cascade by dopamine in renal epithelial cells is fully dependent on hydrogen peroxide generation by monoamine oxidases, J. Am. Soc. Nephrol. 14 (2003) 855–862.
[48] T. Nakano, T. Nagatsu, H. Higashida, Expression of A and B types of monoamine oxidase in differentiated neuroblastoma hybrid cells, J. Neurochem. 44 (1985) 755–758.
[49] E.D. Roberson, J.D. English, J.P. Adams, J.C. Selcher, C. Kondratick, J.D. Sweatt, The mitogen-activated protein kinase cascade couples PKA and PKC to cAMP response element binding protein phosphorylation in area CA1 of hippocampus, J. Neurosci. 19 (1999) 4337–4348.
[50] D. Salat, E. Tolosa, Levodopa in the treatment of Parkinson's disease: current status and new developments, J. Park. Dis. 3 (2013) 255–269.
[51] L. Dezsi, L. Vecsei, Monoamine oxidase B inhibitors in Parkinson's disease, CNS Neurol. Disord. Drug Targets 16 (2017) 425–439.
[52] K.C. Teo, S.-L. Ho, Monoamine oxidase-B (MAO-B) inhibitors: implications for disease-modification in Parkinson's disease, Transl. Neurodegener. 2 (2013) 19.
[53] R.S. Friese, P. Mahboubi, N.R. Mahapatra, S.K. Mahata, N.J. Schork, G.W. Schmid-Schonbein, D.T. O'Connor, Common genetic mechanisms of blood pressure elevation in two independent rodent models of human essential hypertension, Am. J. Hypertens. 18 (2005) 633–652.
[54] V.I. Fedchenko, A.E. Medvedev, Comparative analysis of expression of genes encoding enzymes of catecholamine catabolism and renalase in tissues of normotensive and hypertensive rats, Biomed. Khim. 63 (2017) 312–315.
[55] T. Sagvolden, E.B. Johansen, G. Woien, S.I. Walaas, J. Storm-Mathisen, L.H. Bergersen, O. Hvalby, V. Jensen, H. Aase, V.A. Russell, P.R. Killeen, T. DasBanerjee, F.A. Middleton, S.V. Faraone, The spontaneously hypertensive rat model of ADHD—the importance of selecting the appropriate reference strain, Neuropharmacology 57 (2009) 619–626.
[56] O. Puig, I.M. Wang, P. Cheng, P. Zhou, S. Roy, D. Cully, M. Peters, Y. Benita, J. Thompson, T.Q. Cai, Transcriptome profiling and network analysis of genetically hypertensive mice identifies potential pharmacological targets of hypertension, Physiol. Genomics 42A (2010) 24–32.
[57] R.W. Fuller, S.K. Hemrick-Luecke, Mechanisms of MPTP (1-methyl-4-phenyl-1,2,3,6-tetrahydropyridine) neurotoxicity to striatal dopamine neurons in mice, Prog. Neuro-Psychopharmacol. Biol. Psychiatry 9 (1985) 687–690.
[58] J.W. Langston, I. Irwin, E.B. Langston, L.S. Forno, Pargyline prevents MPTP-induced parkinsonism in primates, Science 225 (1984) 1480–1482.
[59] A. Maertens, T. Luechtefeld, A. Kleensang, T. Hartung, MPTP's pathway of toxicity indicates central role of transcription factor SP1, Arch. Toxicol. 89 (2015) 743–755.
[60] L. Yao, X. Dai, Y. Sun, Y. Wang, Q. Yang, X. Chen, Y. Liu, L. Zhang, W. Xie, J. Liu, Inhibition of transcription factor SP1 produces neuroprotective effects through decreasing MAO B activity in MPTP/MPP(+) Parkinson's disease models, J. Neurosci. Res. (2018), https://doi.org/10.1002/jnr.24266.
[61] Q.Y. Ye, X.D. Zhang, B.X. Huang, Y.G. Zhu, X.C. Chen, Astaxanthin suppresses MPP+-induced oxidative damage in PC12 cells through a Sp1/NR1 signaling pathway, Mar. Drugs 11 (2013) 1019–1034.
[62] Q. Yu, Q. Huang, X. Du, S. Xu, M. Li, S. Ma, Early activation of Egr-1 promotes neuroinflammation and dopaminergic neurodegeneration in an experimental model of Parkinson's disease, Exp. Neurol. 302 (2018) 145–154.
[63] C. Vizcaino, L.E. Nunez, F. Moris, J. Portugal, Genome-wide modulation of gene transcription in ovarian carcinoma cells by a new mithramycin analogue, PLoS One 9 (2014), e104687.
[64] A. Kalyani, P.J. Sonawane, A.A. Khan, L. Subramanian, G.B. Ehret, A.S. Mullasari, N.R. Mahapatra, Post-transcriptional regulation of renalase gene by miR-29 and miR-146 microRNAs: implications for cardiometabolic disorders, J. Mol. Biol. 427 (2015) 2629–2646.
[65] P.J. Sonawane, B.S. Sahu, B.K. Sasi, P. Geedi, G. Lenka, N.R. Mahapatra, Functional promoter polymorphisms govern differential expression of HMG-CoA reductase gene in mouse models of essential hypertension, PLoS One 6 (1) (2011), e16661.

[66] M. Jordan, F. Wurm, Transfection of adherent and suspended cells by calcium phosphate, Methods 33 (2004) 136–143.
[67] B.K. Sasi, P.J. Sonawane, V. Gupta, B.S. Sahu, N.R. Mahapatra, Coordinated transcriptional regulation of Hspa1a gene by multiple transcription factors: crucial roles for HSF-1, NF-Y, NF-kappaB, and CREB, J. Mol. Biol. 426 (2014) 116–135.
[68] M.P. Gupta, M. Gupta, R. Zak, V.P. Sukhatme, Egr-1, a serum-inducible zinc finger protein, regulates transcription of the rat cardiac alpha-myosin heavy chain gene, J. Biol. Chem. 266 (1991) 12813–12816.
[69] A. Riccio, S. Ahn, C.M. Davenport, J.A. Blendy, D.D. Ginty, Mediation by a CREB family transcription factor of NGF-dependent survival of sympathetic neurons, Science 286 (1999) 2358–2361.
[70] S. Liu, Z. Liu, Z. Xie, J. Pang, J. Yu, E. Lehmann, L. Huynh, T. Vukosavljevic, M. Takeki, R.B. Klisovic, R.A. Baiocchi, W. Blum, P. Porcu, R. Garzon, J.C. Byrd, D. Perrotti, M.A. Caligiuri, K.K. Chan, L.C. Wu, G. Marcucci, Bortezomib induces DNA hypomethylation and silenced gene transcription by interfering with Sp1/NF-kappaB-dependent DNA methyltransferase activity in acute myeloid leukemia, Blood 111 (2008) 2364–2373.
[71] J. Ma, Z. Ren, Y. Ma, L. Xu, Y. Zhao, C. Zheng, Y. Fang, T. Xue, B. Sun, W. Xiao, Targeted knockdown of EGR-1 inhibits IL-8 production and IL-8-mediated invasion of prostate cancer cells through suppressing EGR-1/NF-kappaB synergy, J. Biol. Chem. 284 (2009) 34600–34606.
[72] K.M. Walton, R.P. Rehfuss, J.C. Chrivia, J.E. Lochner, R.H. Goodman, A dominant repressor of cyclic adenosine 3′,5′-monophosphate (cAMP)-regulated enhancer-binding protein activity inhibits the cAMP-mediated induction of the somatostatin promoter in vivo, Mol. Endocrinol. 6 (1992) 647–655.